ROYAL SOCIETY OPEN SCIENCE

royalsocietypublishing.org/journal/rsos

Review

Cite this article: Mensah MB, Lewis DJ, Boadi NO, Awudza JAM. 2021 Heavy metal pollution and the role of inorganic nanomaterials in environmental remediation. *R. Soc. Open Sci.* **8**: 201485.
https://doi.org/10.1098/rsos.201485

Received: 21 May 2021
Accepted: 14 September 2021

Subject Category:
Chemistry

Subject Areas:
environmental chemistry/nanotechnology/inorganic chemistry

Keywords:
pollution, heavy metals, environmental remediation, inorganic nanomaterials, adsorption

Author for correspondence:
Michael B. Mensah
e-mails: michael.mensah@knust.edu.gh, mike_baa@yahoo.com

This article has been edited by the Royal Society of Chemistry, including the commissioning, peer review process and editorial aspects up to the point of acceptance.

Electronic supplementary material is available online at https://doi.org/10.6084/m9.figshare.c.5646892.

ROYAL SOCIETY OF CHEMISTRY

THE ROYAL SOCIETY PUBLISHING

Heavy metal pollution and the role of inorganic nanomaterials in environmental remediation

Michael B. Mensah[1], David J. Lewis[2], Nathaniel O. Boadi[1] and Johannes A. M. Awudza[1]

[1]Department of Chemistry, Kwame Nkrumah University of Science and Technology, PMB, Kumasi, Ghana[2]Department of Materials, University of Manchester, Oxford Road, M13 9PL, UK

MBM, 0000-0002-8080-4812

Contamination of water and soil with toxic heavy metals is a major threat to human health. Although extensive work has been performed on reporting heavy metal pollutions globally, there are limited review articles on addressing this pernicious phenomenon. This paper reviews inorganic nanoparticles and provides a framework for their qualities required as good nanoadsorbents for efficient removal of heavy metals from water. Different inorganic nanoparticles including metals, metal oxides and metal sulfides nanoparticles have been applied as nanoadsorbents to successfully treat water with high contaminations of heavy metals at concentrations greater than 100 mg l^{-1}, achieving high adsorption capacities up to 3449 mg g^{-1}. It has been identified that the synthesis method, selectivity, stability, regeneration and reusability, and adsorbent separation from solution are critical parameters in deciding on the quality of inorganic nanoadsorbents. Surface functionalized nanoadsorbents were found to possess high selectivity and capacity for heavy metals removal from water even at a very low adsorbent dosage of less than 2 g l^{-1}, which makes them better than conventional adsorbents in environmental remediation.

1. Introduction

Pollution of water and soil is a global concern. Heavy metals such as mercury (Hg), lead (Pb), cadmium (Cd) and arsenic (As) are highly poisonous and their pollution even at low concentrations in water and soil poses a serious threat to the health of humans and other terrestrial animals. Mercury has deleterious effects on the human kidney, brain and central nervous system, whereas

lead pollution has been associated with neurodevelopmental effects, and cadmium is classified as a carcinogen [1,2]. Arsenic intake causes dermal lesions, skin cancers, bladder and lung cancers [1]. To mitigate these health effects, the World Health Organization (WHO) has set recommended levels for Hg, Pb, Cd and As in drinking water to be 0.006, 0.01, 0.003 and 0.01 mg l^{-1}, respectively [1]. The reported major source of mercury contamination in most developing countries is the proliferation of illegal artisanal gold mining activities in which mercury-gold amalgamation methods are used [3–5]. Manufacturing of batteries, steel, plastics and fertilizers, and mining are the common sources of the exposure of lead and cadmium to the environment. Arsenic contamination is predominant in underground waters where sulfide and sedimentary deposits are present [1].

Mercury is volatile and, predominantly, exists as Hg^{2+} in water [6,7]. The Hg^{2+} ion is highly toxic even at low concentrations and can accumulate in ecosystems, in particular apex predators, causing several disorders and diseases. Methyl mercury (CH_3Hg^+) is another form of mercury that bioaccumulates in organic tissues, poisoning the food chain [8,9]. The Minamata Convention on Mercury established in October 2013 saw over 130 countries signing, and declared mercury pollution as a global problem that no country can solve alone is a classic example of food poisoning by heavy metals [10]. This convention was inspired by a fishing village near Minamata city in Japan, which drew the world's attention to the devastating effects of mercury as a powerful neurotoxicant that is known to dangerously affect fetuses, infants and young children. A local chemical factory was eventually found responsible for discharging mercury waste into the Shiranui Sea which killed fishes and other sea creatures and mysteriously, affected several families that ate contaminated seafoods. Children were diagnosed with cerebral palsy and eventually with what was known as the Minamata disease. The disaster is outlined by Kessler [10].

Inorganic lead (Pb^{2+}) compounds are the most predominant forms of lead in the environment. The highly toxic organic lead compounds, associated with the historic use of leaded gasoline and paints have been phased out [11]. Cadmium ions (Cd^{2+}), primarily, exists as greenockite (hexagonal cadmium sulfide, CdS) and usually occurs in association with zinc [12]. Arsenic is associated with gold ores and exists in different oxidation states (−3, 0, +3 and +5) and in water, the As^{5+} form (arsenate) is predominant [1].

Significant research has been reported widely on the levels of contamination of heavy metals in the environment, and these lay the foundation for developing sequestration strategies for remediation. For example, Ghana being an African country where mining and quarrying activities are predominant, the levels of Hg, Pb, Cd and As pollution in water bodies, sediments and soils reported from 2003 to 2018, ranged from 0.001 µg l^{-1}–19.82 mg l^{-1}, 0.001–93.10 mg kg^{-1} and 0.0011–57.80 mg kg^{-1} of Hg, 0.012 µg l^{-1}–11.60 mg l^{-1}, 0.005–307.20 mg kg^{-1} and 1.025–571.3 mg kg^{-1} of Pb, 0.006 µg l^{-1}–1.4 mg l^{-1}, 0.00015–90.50 mg kg^{-1} and 0.0011–103.66 mg kg^{-1} of Cd and 0.011 ug l^{-1}–18.40 mg l^{-1}, 0.00197–10 200 mg kg^{-1} and 0.08–18.60 mg kg^{-1} of As, respectively [13–70]. The source of pollution has been largely attributed to illegal artisanal gold mining activities.

Heavy metal removal strategies from water include chemical precipitation, ion exchange, solvent extraction, cloud point extraction, ultrafiltration, reverse osmosis, crystallization, evaporation, photocatalysis and adsorption techniques. Apart from adsorption, the rest of the techniques suffer disadvantages such as (i) sludge production, (ii) high energy requirements, (iii) high operational costs, (iv) requirement for the use of solvents, (v) possible inefficiency at removing trace concentrations of some toxic metal ions, (vi) solubility limitations, (vii) possible use of high-pressure operations, and (viii) requirement of expensive analytical instrumentation [8,71–74]. However, the adsorption technique is simple and effective; the adsorbents are usually easy to handle, and the operation and design are flexible [8,75].

The most common materials used as adsorbents for heavy metals sequestration are activated carbon, zeolite, silica gel, activated alumina, natural clay (kaolinite, bentonite, illite, stevensite and rectorite) and biomass [9,73]. Silica has been shown to possess a surface area of 200–1500 m^2 g^{-1} and, together with its porous nature, appears to be a very good adsorbent for heavy metal remediation [9]. Activated carbon with a surface area of 2082 m^2 g^{-1} has been shown to display the maximum adsorption capacity of 56.2–135.8 mg g^{-1} over other equally good adsorbent systems [76]. Although these adsorbent materials are suitable, they lack selectivity and have a poor affinity towards targeted heavy metals. With the advent of nanoscience, which involves techniques for scaling down sizes of materials to the nanoscale (1–100 nm), adsorbents can be designed to possess enhanced properties compared with common bulk material adsorbents.

Nanoscale adsorbents offer better selectivity, capacity and improved affinity towards heavy metals pollutants and also provide faster and efficient adsorption processes [77]. In addition, nanoscale

adsorbents possess (i) high surface area to volume ratio, (ii) surface functional groups tailored for a specific application, (iii) short diffusion route or absence of internal diffusion resistance, (iv) high porosity, (v) enhanced structural properties, and (vi) catalytic properties [8,72,73,77–79]. These properties make nanoadsorbents highly selective, and with the capacity to achieve efficient adsorption of a variety of water pollutants including heavy metals. Examples of useful nanoadsorbents are zero-valent iron (n-ZVI), iron oxide (Fe_3O_4), Fe_3O_4@SiO_2-SH, iron sulfide (FeS), amorphous silica (SiO_2) and aluminium-silicate-mixed oxides nanomaterials. Interestingly, blends of inorganic nanomaterials with large surface area metal-organic frameworks (MOFs) and covalent organic frameworks (COFs) have shown high adsorption capacity for heavy metals and radionuclides [80,81].

This review covers several key areas including the different types of inorganic nanoparticles useful as adsorbent materials and the potential qualities of nanoparticles required for efficient removal of heavy metals from solution. This knowledge is essential for the design of efficient nanoadsorbents with capacities to remove heavy metals at levels prevailing in the environment and subsequently providing improvement to water treatment strategies, especially in mining areas.

2. Inorganic nanomaterials used as adsorbents

Nanomaterials are nanoscale materials with improved performance relative to the bulk material, often called emergent properties. Nanoscale materials due to the size effect emanating from the quantum confinement can be used as efficient adsorbents for environmental remediation processes. Nanomaterials span a variety of materials including inorganic, carbon-based, polymer, nanocomposites and biomaterials. In environmental remediation, inorganic nanomaterials have been widely applied [82]. Table 1 shows the characteristics and adsorption capacities of some inorganic nanoadsorbents for removal of Hg, Pb, Cd and As ions from solution.

2.1. Metal nanoparticles

Metal nanoparticles employed for the removal of heavy metals include Au, Ag and nano-zero-valent iron (n-ZVI) nanoparticles [7,104,105]. To improve the selectivity of some common adsorbents such as silica, alumina and activated carbon, Au and Ag metal nanoparticles have been used together with these materials to form composites or core–shell nanostructured materials [9,105,106]. Solis *et al*. [9] compared the adsorption capacities of a 3.19 nm size Au metal nanoparticle coated on silica and sand and found that the former showed a high affinity towards adsorption of Hg from water with K_D (partition coefficient, which is a measure of sorbent affinity towards adsorbate) value of 9.96 l g^{-1} and adsorption efficiency of 96%. This confirmed the successful deposition of 6.9 mg of Au nanoparticles on a gram of silica compared with the sand which had only 1.5 mg deposition. The high selectivity was possible because Au forms a stable amalgam with Hg in the form of Au_3Hg. The Au_3Hg alloy is thermodynamically favourable at room temperature, and thus, the mercury adsorbed was directly proportional to the Au content in the silica [104]. Other metals like Ag, Al and Cu also form amalgams with Hg [6,7,104]. The adsorption capacities of Au and Ag metal nanoparticles can be less than or equal to 800 mg g^{-1} which is comparable to metal oxides but may be relatively expensive [9,105].

2.2. Nano-zero-valent iron

Nano-zero-valent iron (n-ZVI) is a very promising metal nanoparticle that is gaining much interest as nanoadsorbents for a wide range of water pollutants including heavy metals [7]. The n-ZVI consists of an inner zero-valent iron Fe^0 core and an outer mixed iron oxides shell layer [7]. The core acts on the source of contaminants through electrostatic interaction and surface complexation [7]. The n-ZVI with a surface area of 26.3 m^2 g^{-1} and a wide range of particle sizes between 20 and 200 nm ensured the adsorption of Cd^{2+} ions from an aqueous solution up to the tune of 769.2 mg g^{-1} [94]. Making a similar composite with activated carbon led to a low adsorption capacity of 142.8 mg g^{-1} for Cd^{2+} [107]. Compositing 10 nm n-ZVI particle with graphene also ensured the removal of Pb^{2+} from aqueous solution with an adsorption capacity of 585 mg g^{-1} [108]. In addition to the adsorption of Pb^{2+}, the n-ZVI reduces Pb^{2+} to Pb^0, and this ensures the easy magnetic separation from solution [108]. However, there are possible handling challenges with n-ZVI, since it is highly reactive and may be toxic [109].

Table 1. Some nanoadsorbents were reported for the adsorption of Hg, Pb, Cd and As from an aqueous solution. LCMED: L-cysteine methyl ester dendrimer, HA: humic acid, Ga: glutaraldehyde, Cs: chitosan, CMC: carboxymethyl cellulose, L: SiO_2, lauric acid, oleic acid, multi-walled carbon nanotubes (MWCNTs), L-arginine, mesoporous silica, hydroxyapatite or ethylenediaminetetraacetic acid (EDTA), L-cyst.: L-cysteine, APTES: (3-aminopropyl)triethoxysilane, n-ZVI: nano-zero-valent iron, OPP: orange peel powder, Sd: sawdust, SdC: sawdust carbon, ZIF-8: zeolitic imidazolate framework-8, AA: ascorbic acid.

adsorbent	surface area ($m^2\ g^{-1}$)	dose ($g\ l^{-1}$)	target heavy metal ion	metal ion conc. ($mg\ l^{-1}$)	pH	adsorption capacity ($mg\ g^{-1}$)	ref.
Al_2O_3-SiO_2-LCMED	73.6	1	Hg(II)	5–4000	6	3232	[71]
Fe_3O_4-HA	64	0.1	Hg(II)	1	6	97.7	[83]
Fe_3O_4-Ga-Cs	<3	1	Hg(II)	100	5–6	152	[84]
CuO	89.59	0.05	Hg(II)	10–100	9	825.21	[85]
FeS-CMC	36.9	0.0025	Hg(II)	4.8–40	6.5–10.5	3449	[86]
ɣ-Fe_2O_3	79.35	10	Pb(II)	1–20	5	68.90	[87]
ɣ-Fe_2O_3@L	74–214	0.55	Pb(II)	40–50	7	49.30–88.2	[88]
Fe_3O_4@L-cyst.	58.49	2	Pb(II)	50	6	18.78	[89]
SiO_2@APTES	390	1	Pb(II)	100	3	40.40	[90]
MnO_2-MWCNTs	6.4	1	Pb(II)	10	7	20	[91]
MgO	72	0.67	Pb(II)	100	7	1980	[92]
SnO_2	24.48	0.25	Pb(II)	100–400	4–7	1265.8	[93]
n-ZVI	26.3	0.5	Cd(II)	25–450	—	769.2	[94]
Fe_3O_4@OPP	65.19	0.2	Cd(II)	16	7	76.92	[95]
Fe_3O_4-SdC@EDTA	14	0.4	Cd(II)	30	6.5	63.30	[96]
Fe_3O_4@Sd	51.36	0.2	Cd(II)	50–250	7	1000	[97]
SiO_2@APTES	390	1	Cd(II)	100	6	49.46	[90]
MgO	72	0.67	Cd(II)	100	7	1500	[92]
SnO_2	24.48	0.25	Cd(II)	100–400	4–7	1275.5	[93]
ZnO	8.25	0.4	Cd(II)	20–140	7	214.4	[98]
ZrO_2	327	≤0.15	As(III)	0.3–100	7	83	[99]
$MnFe_2O_4$	197.39	2	As(V)	10–400	2.1	68.25	[100]
ZIF-8	1063.5	0.2	As(V)	20	7	60.03	[101]
ɣ-Fe_2O_3	90.4	0.06	As(V)	1–11	3	50	[102]
Fe_3O_4-AA	179	0.06	As(III)	1	7	46.06	[103]

2.3. Magnetic metal oxide nanoparticles

The most widely used magnetic metal oxides are iron oxides. Their vast application as nanoadsorbents emanates from the possibility of rapidly separating them from solution using an external magnet [110]. Iron oxides including magnetite (Fe_3O_4), haematite (Fe_2O_3), maghaemite (ɣ-Fe_2O_3), goethite (α-FeO(OH)), lepidocrocite (ɣ-FeO(O)), manganese-doped iron oxide ($MnFe_2O_4$) and mixed iron oxides have been used for the adsorption of Pb^{2+}, Cd^{2+} and Hg^{2+} ions from aqueous solutions [88,109,111–113]. Bare iron oxides have shown adsorption capacities ranging 1.69–101.1 and 0.1105–820.16 $mg\ g^{-1}$ for Cd^{2+} and Pb^{2+}, respectively [109,112,114–116]. Goethite and lepidocrocite as two different phases of iron oxide/hydroxide have shown high adsorption capacities of 820.16 and 527.94 $mg\ g^{-1}$, respectively, for Pb^{2+} due to the OH surface groups on their surfaces which bind strongly with Pb^{2+} [112]. Manganese-doped iron oxide ($MnFe_2O_4$) nanoparticles also have been shown to possess high adsorption

capacities of 488, 97 and 136 mg g^{-1} for Pb^{2+}, As^{3+} and As^{5+}, respectively [117]. The use of Fe_3O_4@C@MnO_2 for removal of Eu(III)/U(VI), X-ray photoelectron spectroscopy and zeta potential analyses showed that the adsorption process was governed by surface complexation and electrostatic attraction [118].

The superparamagnetic nature of iron oxides coupled with the nanoscale capabilities makes them excellent adsorbent materials. In addition, iron oxide surfaces in many other studies were functionalized with suitable functional groups aimed at improving their selectivity towards targeted pollutants. Lauric acid, oleic acid, L-arginine, ethylenediaminetetraacetic acid, sulfo (SO_3H), maleate, humic acid (HA), polyrhodamine and 2-mercapto benzothiazole-capped iron oxide nanoparticles have been used for the removal of Cd^{2+}, Pb^{2+} and Hg^{2+} from aqueous solution [78,88,110,119,120]. These functionalized iron oxides afforded an adsorption capacity range of 0.59–108.93 mg g^{-1}. Compositing iron oxide with silica or chitosan with further functionalization with thiol and glutaraldehyde resulted in Hg^{2+} adsorption capacities of 148.8 and 152 mg g^{-1}, respectively [84,121]. Interestingly, Fe_3O_4 nanoparticles coated with natural biodegradable materials such as sawdust, orange peel powder, cashew nutshell resin and shellac (natural resin with abundant hydroxyl and carboxylic groups) have been used for the adsorption of Cd^{2+} [95–97,122,123]. Sawdust-coated Fe_3O_4 nanoparticle with BET active surface area of 51.36 m^2 g^{-1} incredibly removed Cd^{2+} from 50 to 250 mg l^{-1} Cd^{2+} aqueous solution, and the adsorption capacity was reported to be 1 g g^{-1} [97]. However, Fe_3O_4 coated with shellac, orange peel powder, and sawdust carbon showed relatively lower Cd^{2+} adsorption capacities of 18.8, 76.92 and 63.3 mg g^{-1}, respectively [95,96,122]. Irrespective of the various functionalization treatments, iron oxides maintained their magnetic properties which enable them to be separated from the solution.

2.4. Other metal oxide nanoparticles

Apart from iron oxide, nanoparticles of metal oxides such as silica (SiO_2), alumina (Al_2O_3), magnesium oxide (MgO), caesium oxide (CeO_2), titanium dioxide (TiO_2), tin oxide (SnO_2), zinc oxide (ZnO), manganese dioxide (MnO_2), copper oxide (CuO), nickel oxide (NiO_2) and zirconium oxide (ZrO_2) have been used as nanoadsorbents for sequestration of heavy metals from water. Table 1 shows adsorption conditions and capacities of different metal oxide nanoadsorbent for Hg^{2+}, Cd^{2+}, Pb^{2+} and As^{3+}.

Amorphous silica is non-toxic, has a high specific surface area and regular pore structures, making it a very promising adsorbent material [73]. Aminopropyl-functionalized silica nanoparticles with an average size of 7 nm possessed a large BET surface area of 390 ± 40 m^2 g^{-1} and could adsorb 0.44 (49.46) and 0.195 (40.40) mmol g^{-1} (mg g^{-1}) of Cd^{2+} and Pb^{2+}, respectively [90]. Arce *et al*. [90] confirmed using DFT quantum computational calculations the formation of Pb-N and Pb-C bond distances which strongly agree with the extended X-ray absorption fine structure data. Alumina with a particle size of approximately, 6–13 nm adsorbed Pb^{2+} at 47.08 mg g^{-1} capacity [124]. Mixed oxides of silica and alumina nanoparticles functionalized with L-cysteine methyl ester dendrimer demonstrated an incredible adsorption capacity of 3232 mg g^{-1} for Hg^{2+} [71]. Figure 1 shows the morphology and performance of the L-cysteine methyl ester dendrimer-coated mixed oxides of silica and alumina nanoparticles. Alumina-silicate-mixed oxides are resistant to oxidation, chemically and thermally stable and have high conductivity, low dielectric constant, creep resistant and low thermal expansion [71].

Nanoparticles of CuO and ZnO also have high adsorption capacities for Hg^{2+}. Fakhri [85] and Sheela *et al*. [126] reported CuO and ZnO adsorption capacities of approximately 825.21 and 714 mg g^{-1}, respectively, for Hg^{2+}. The high adsorption of CuO may be that Cu forms a stable amalgam with Hg^{2+} [104]. SnO nanoparticles are conducting, transparent and gas-sensitive, and thus, are gaining much interest as nanoadsorbents and as catalysts. SnO with a surface area of 24.48 m^2 g^{-1} as measured by BET isotherms demonstrated adsorption of Pb^{2+} and Cd^{2+} at 1265.8 and 1275.5 mg g^{-1}, respectively [93]. Flowerlike MgO nanostructures also displayed excellent adsorption of Pb^{2+} and Cd^{2+}. Figure 2 shows the TEM images and adsorption isotherms of the flowerlike MgO nanostructures. With a BET surface area of 72 m^2 g^{-1}, MgO was able to remove Pb^{2+} and Cd^{2+} ions from 100 mg l^{-1} metal ions solution at adsorption capacities of 1980 and 1500 mg g^{-1}, respectively [92]. The adsorption mechanism exhibited by MgO is ion exchange, leaving some level of Mg^{2+} in solution. However, Mg^{2+} is not toxic and the recommended level in drinking water is 450 mg l^{-1} according to WHO [92]. We note that there appear to be very few reports on the use of CuO, ZnO, SnO and MgO nanoparticles for heavy metal sequestration. Though they possess impressive heavy metals adsorption capacities, their removal from the solution will still be a challenge. To impart magnetization to these materials, in order to ensure simplicity of removal from solution using an

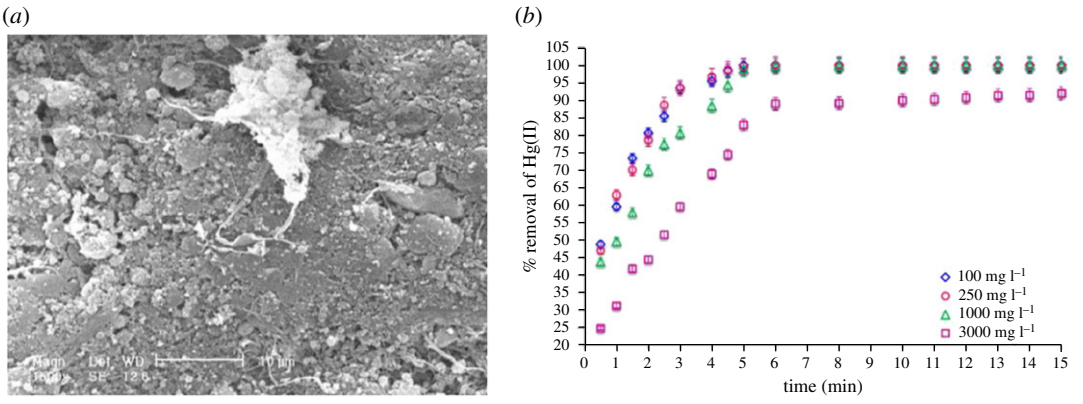

Figure 1. (*a*) SEM images of mixed oxides of silica and alumina nanoparticle functionalized with L-cysteine methyl ester dendrimer and (*b*) its adsorption kinetics for the adsorption of Hg(II) ions at different concentrations. Reprinted with permission from Arshadi *et al*. [71]. Copyright (2021) Elsevier.

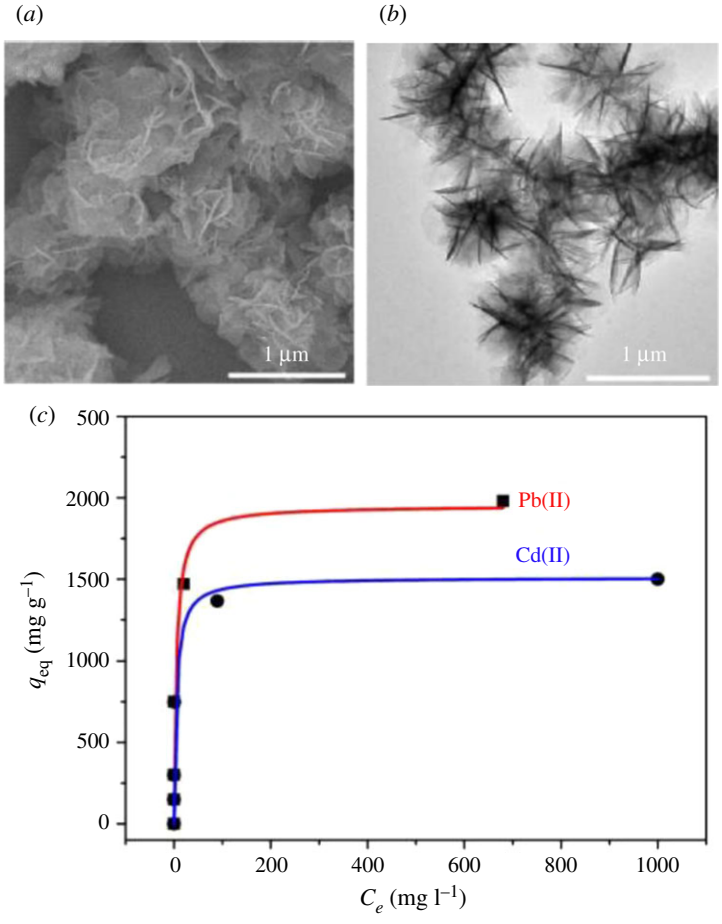

Figure 2. TEM image (*a*) low-magnification and (*b*) high-magnification of flowerlike MgO nanostructures, and (*c*) Pb(II) and Cd(II) adsorption isotherms obtained using flowerlike MgO nanostructures. Reprinted with permission from Cao *et al*. [92]. Copyright (2021) American Chemical Society.

external magnet, doping with Fe and Mn could potentially be a strategy to impart these magnetic properties to the host material.

2.5. Metal sulfide nanoparticles

Compared with metal oxides, metal sulfides often possess a superior affinity for heavy metal ions; however, they have received less attention as nanoadsorbents for heavy metal removal from water

[128]. Metal sulfides remove divalent metal ions through (i) chemical precipitation (equation (2.1)), (ii) ion exchange (equation (2.2)), and (iii) complexation (equation (2.3)) [86]. The most studied metal sulfide as adsorbent for heavy metals removal is iron sulfide (FeS) or mackinawite.

$$\mathrm{MS(s)} + \mathrm{A^{2+}(aq)} \rightarrow \mathrm{AS(s)} + \mathrm{M^{2+}(aq)}, \tag{2.1}$$

$$\mathrm{MS(s)} + \mathrm{xA^{2+}(aq)} \rightarrow [M_{(1-x)}, \mathrm{A_x}]\ \mathrm{S(\ s)} + \mathrm{xM^{2+}(aq)}, \quad (x < 1) \tag{2.2}$$

and

$$\mathrm{MS(s)} + \mathrm{A^{2+}(aq)} \rightarrow \mathrm{MS} - - - - - \mathrm{A^{2+}}. \tag{2.3}$$

FeS naturally scavenges for Hg^{2+} and forms stable β-HgS (metacinnabar, with solubility product, K_{sp}, 4×10^{-54}) even in the presence of organic matter [86]. FeS also removes divalent metal ions such as Mn^{2+}, Ca^{2+}, Mg^{2+}, Ni^{2+} and Cd^{2+}. Additionally, FeS is a reductant and acts as an electron donor, making it possible to reduce and detoxify chlorinated organic compounds and inorganic oxyanions of Cr(VI), Se(VI) and As(VI) [129]. Remarkably, carboxymethyl cellulose (CMC)-stabilized FeS offered an Hg^{2+} sorption capacity of 3449 mg g^{-1}, and this was attributed to the dual-mode sorption mechanism where CMC-FeS adsorbs Hg^{2+} through concurrent precipitation [86]. Similarly, a large Pb^{2+} remediation capacity of 2950 mg g^{-1} has been demonstrated by Pala & Brock [128] with zinc sulfide (ZnS) gel, where the mechanism is mainly more of ion exchange than adsorption. ZnS has been successfully used to sequentially remove Hg^{2+}, Cu^{2+}, Pb^{2+} and Cd^{2+} from simulated contaminated water containing 5–678 mg l^{-1} of heavy metal ions at removal efficiencies of 99.9%, 99.9%, 90.8% and 66.3%, respectively [77]. The ZnS showed higher selectivity towards Hg^{2+} and Cu^{2+} than Pb^{2+} and Cd^{2+}, and this Fang *et al.* [77] attributed to the differences in the solubility product (K_{sp}) of the metal sulfides. The lower the K_{sp}, the higher the stability of the sulfide, and hence, the higher the precipitation and adsorption. The selectivity of the sulfides may also be attributed to the hard–soft acids and bases (HSAB) theory pioneered by Pearson (vide infra), where the sulfur which is a soft base will have a higher affinity for Hg^{2+} which is a soft acid. However, adequate research will be required to clearly establish the mechanism of metal sulfides selective adsorption.

Core–shell nanostructured materials, such as Fe_3O_4-ZnS combines the magnetic properties of the iron oxide and the better affinity of ZnS, making sure that adsorbent material is easily separable and also selective. The magnetic Fe_3O_4-ZnS nanoparticles gave an adsorption capacity of 129.9 mg g^{-1} for removal of Hg^{2+} from water which is better compared with non-magnetic adsorbents [130].

The different nanomaterials discussed above for heavy metals sequestration have unique advantages and disadvantages (table 2). Thus, a search for new inorganic nanoadsorbents with efficient and robust properties or qualities is desired.

3. Qualities of nanoadsorbents

The qualities of nanoparticles that make them suitable as nanoadsorbents for sequestration of heavy metals include (i) simple and cheap synthesis pathway, (ii) selectivity and affinity towards the target pollutant, (iii) thermal and chemical stability in solution, (iv) ease of removal from solution after adsorption, (v) it should be easily regenerated and re-used severally, and (vi) should have the ability to perform other functions apart from adsorption.

3.1. Synthesis pathway

The synthetic pathways generally reported for nanoadsorbent synthesis usually include (i) reduction, (ii) co-precipitation, (iii) sol–gel, and (iv) hot-injection methods. Figure 3 shows the different synthesis pathways for nanoadsorbent synthesis.

3.1.1. Reduction

The reduction route is often employed for the synthesis of metal nanoparticles such as Au, Ag and n-ZVI. Ojea-Jiménez *et al.* [104] synthesized Au nanoparticles (with size 8.9 ± 1.6 nm) by reducing Au^{3+} with sodium citrate ($Na_3C_6H_5O_7$) and was able to achieve 100% of Hg removal from water; however, the initial concentration of Hg was only 0.16 ppm. Similarly, Lisha and Pradeep [132] synthesized Au nanoparticles by using $Na_3C_6H_5O_7$ to reduce Au^{3+} to Au^0 nanoparticles and further supported it with alumina, resulting in Hg adsorption capacity of 4.065 g g^{-1}. Sodium borohydride ($NaBH_4$) has also been used to reduce Ag^+ to Ag^0 nanoparticles for adsorption of Hg [105]. Using $NaBH_4$, Yan *et al.* [7]

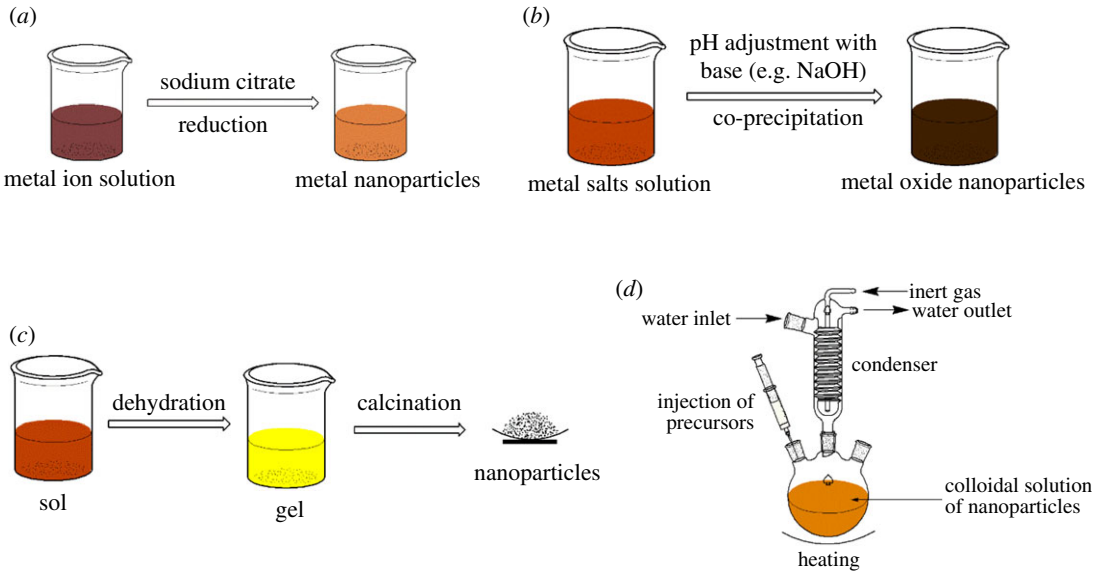

Figure 3. Synthesis pathways for nanoadsorbents: (*a*) reduction, (*b*) co-precipitation, (*c*) sol–gel and (*d*) hot-injection methods.

Table 2. Advantages and disadvantages of nanoadsorbent materials.

nanoparticle	advantages	disadvantages	ref.
metal	– forms stable amalgam with heavy metal pollutant (e.g. Hg)	– relatively expensive	[9,105]
n-ZVI	– adsorbs wide range of water pollutants – possesses reductive potential – highly reactive	– has handling challenges – may be toxic	[109]
magnetic metal oxide	– rapid separation from aqueous solution using an external magnet	– has relatively low adsorption capacity for heavy metals – requires functionalization to improve adsorption capacity	[87,97]
non-magnetic metal oxide	– has high adsorption capacity for heavy metals (e.g. CuO, ZnO, SnO, MgO)	– possible challenges with separation from aqueous solutions	[71,92]
metal sulfide	– possesses specific affinity for heavy metals adsorption	– prone to oxidation	[131]

synthesized n-ZVI nanoparticles, which were able to adsorb 98% of Hg from 40 mg l^{-1} Hg solution within 2 min. Sodium citrate and $NaBH_4$ are efficient reducing agents commonly used in nanoparticles synthesis. While sodium citrate is food grade and biologically compatible, $NaBH_4$ introduces boron into the water which could raise public health concerns.

3.1.2. Co-precipitation

In co-precipitation synthesis, the solutes are usually soluble at a particular condition but precipitate out of solution when supersaturation is reached. Co-precipitation is simple and rapid, provides easy control of the particle size and composition, provides the possibility of nanoparticle surface modification, is energy-efficient, and does not require organic solvents. However, co-precipitation could yield impure nanoparticles with irregular and less homogenized nanoparticle sizes; it is time-consuming and has poor reproducibility [133]. Fe_3O_4 has been synthesized widely using the co-precipitation technique, largely due to its simplicity and easiness of modification of the nanoparticle surface. Mehdinia *et al.* [2] synthesized Fe_3O_4 nanoparticles using co-precipitation, supported it with silica and functionalized the surface with dithiocarbamate, which resulted in approximately 99% adsorption of Hg from water.

Similarly, Fe_3O_4 nanoparticles have been synthesized via co-precipitation and functionalized with glutathione, glutaraldehyde, thiol, polyrhodanine and HA and applied for Hg adsorption from water, affording adsorption capacities between 34.48 and 152 mg g^{-1} [79,83,84,121,134].

3.1.3. Sol–gel synthesis

The sol–gel method employs solvents and chemical reagents that after hydrolysis and condensation, the mixture of solvents turns into a gel. Arshadi *et al.* [71] synthesized SiO_2–Al_2O_3-mixed oxide nanoparticles using the sol–gel method. Typically, the chemical reagents: aluminium tri-sec-butylate and tetraethyl orthosilicate were dissolved in n-butanol and the resultant solution warmed at 60°C. Acetylacetone (H-acac) was added slowly to the solvent mixture after cooling to room temperature to obtain a clear solution. This clear solution was hydrolysed by adding an alkoxide solution and left overnight, resulting in the formation of a transparent gel. The gel was dried to remove the solvents and finally calcined at 500°C to remove the other organic components to obtain the nanoparticles. This nanomaterial was reported to have removed approximately 99.9% of Hg from water with a very high initial Hg concentration of 500 mg l^{-1}. Fakhri [85] also using the sol–gel technique, synthesized CuO nanoparticles which had an Hg adsorption capacity of approximately 825.21 mg g^{-1}. The nanomaterials obtained from the sol–gel method are usually of high purity and porous. Though the sol–gel method gives control over porosity, particle size, chemical composition and dopant incorporation, compared with the other methods, it usually requires longer reaction time and involves organic solvents and higher temperatures to remove the organic components from the gel [133].

3.1.4. Hot-Injection

The hot-injection method involves the injection of a solution of reagents into hot solvents, which gives control over the nucleation and growth of the nanoparticles. It is usually employed for the synthesis of metal chalcogenide nanocrystals. ZnS supported on Al_2O_3 was synthesized using the hot-injection method by Fang *et al.* [77] for the sequential removal of Hg^{2+}, Cu^{2+}, Pb^{2+}, Cd^{2+} and Zn^{2+} in water. The ZnS-Al_2O_3 was prepared by mixing α-Al_2O_3 and $ZnCl_2$ in ethylene glycol in a three-necked flask fitted with a condenser, and maintaining the temperature at 180°C, 1-butylamine solution of thiourea was injected into it continuously, and the resulting mixture aged for 3 h. Although the hot-injection method is efficient and ensures that good quality monodispersed nanoparticles are obtained, it requires a complex set-up and organic solvents, and the resulting nanoparticles' surfaces are already occupied by capping groups or solvents, which makes it unattractive as nanoadsorbents.

Table 3 shows the advantages and disadvantages of the different synthetic methods that have been used for nanoadsorbents syntheses. It must be noted that very few synthetic methods have been explored for the synthesis of nanoadsorbents, and admittedly, this research gap makes it challenging in deciding on suitable synthetic approaches for nanoadsorbents for heavy metals remediation.

3.2. Selectivity and affinity

Activated charcoal is a widely known efficient adsorbent. This is because it is cheap, available and has a high capacity for the removal of a wide range of pollutants. However, activated charcoal is a non-selective adsorbent and has no special affinity towards any specific pollutant. Affinity facilitates the rate of adsorption [9]. This makes nanoadsorbents superior to activated charcoal and other non-specific adsorbents because they could be tailored to possess special affinity and selectivity towards a particular pollutant. Figure 4 shows the chemical structures of compounds used for the functionalization of the nanoparticle surface for improving selectivity towards heavy metals in solution. To improve the preferential adsorption of Hg^{2+} onto SiO_2–Al_2O_3-mixed oxide nanoparticles, Arshadi *et al.* [71] covalently immobilized L-cysteine methyl ester dendrimer onto the surface of the nanoparticle and the selectivity was evaluated in the presence of Pd^{2+}, Pb^{2+}, Cd^{2+}, Zn^{2+}, Cu^{2+}, Co^{2+} and Mn^{2+}. At an initial concentration of 250 mg l^{-1} of metal ions, the functionalized nanoparticles exhibited high selectivity for adsorption of Hg^{2+} of about 96.2%, and low adsorption for the interfering cations at adsorption capacities of 10, 3.7, 1.13, 0.76, 5.81, 1.84 and 3.02%, respectively. However, when the metal cations concentration was increased to 1000 mg l^{-1}, the adsorption of Hg^{2+} decreased to 90%. The selective adsorption was attributed to the –SH and –NH functional groups of the L-cysteine methyl ester which preferentially donated electrons to the Hg^{2+} resulting in complexation [71].

Table 3. Advantages and disadvantages of synthesis methods for nanoadsorbents.

synthesis method	advantages	disadvantages	ref.
reduction	– simple	– some reducing agents may be toxic	[105]
	– suitable for the synthesis of metal nanoparticles		
co-precipitation	– simple and rapid	– yields impure nanoparticles with irregular and less homogenized particle sizes	[133]
	– provides control of particle size and composition	– time-consuming	
	– provides a possibility for nanoparticle surface functionalization	– poor reproducibility	
	– energy efficient		
	– requires no organic solvents		
sol–gel	– yields high purity and porous nanoparticles	– time-consuming	[71,133]
	– provides control over porosity, particle size, composition and dopant incorporation	– involves the use of organic solvent	
		– requires high temperature to remove the organic components from the gel	
hot-injection	– provides control over nucleation and growth of particles	– requires complex set-up	[77]
	– efficient	– requires organic solvents and capping agents	
	– yields monodispersed nanoparticles	– particle surface always covered with capping groups	

Zhang *et al.* [121] demonstrated that thiol-functionalized Fe_3O_4@SiO_2 could selectively remove Hg^{2+} at an adsorption capacity of 110 mg g^{-1} even in the presence of K^+, Na^+ and Ca^{2+} cations which naturally abound in water at high concentrations. While the hydroxyl groups on the surface of the Fe_3O_4@SiO_2 nanoparticle are hard Lewis bases and, therefore, preferred bonding with hard Lewis acids such as alkaline metals and alkaline earth metals, the thiol group being soft Lewis base exhibited a strong preference for bonding with Hg^{2+} which is a soft Lewis acid. Mehdinia *et al.* [2] compared thiol and amine-functionalized magnetic mesoporous silica nanoparticles and found that the thiol functional group was more selective towards Hg^{2+} removal than the amine. Mercury adsorption capacity of 538.9 mg g^{-1} was achieved with the thiol-functionalized nanoparticles, and this was attributed to the thiol functional group. In the presence of competitive cations, the thiol-functionalized nanoparticles were selective to the cations in the order $Hg^{2+} > Pb^{2+} > Cd^{2+} > Zn^{2+}$. This trend was also confirmed by Košak *et al.* [73] when they found mercaptopropyl-functionalized SiO_2 nanoparticles to adsorb 99.9% Hg^{2+}, 55.9% Pb^{2+}, 50.2% Cd^{2+} and 4% Zn^{2+}. Unfortunately, the selectivity of the amine-functionalized nanoparticles was not tested in the presence of the competing cations.

The binding interactions between the carboxylic acid functional groups in free molecules of 2-mercato-4-methyl-5-thiazoleacetic acid (MCT), monomercaptosuccinic acid (MMSA), o-thiosalicylic acid (o-TSA) and p-thiosalicylic acid (p-TSA), and Hg^{2+}, Pb^{2+} and Cd^{2+} cations were explored by Hamid *et al.* [74]. These molecules also contain thiol functional group (figure 4). They realized that the COOH in MCT binds completely (100%) with the Pb^{2+} and Cd^{2+}, and only 20% with Hg^{2+}; the COOH in MMSA binds 97% with Pb^{2+}, 91% with Cd^{2+} and had no interaction with Hg^{2+}; the COOH

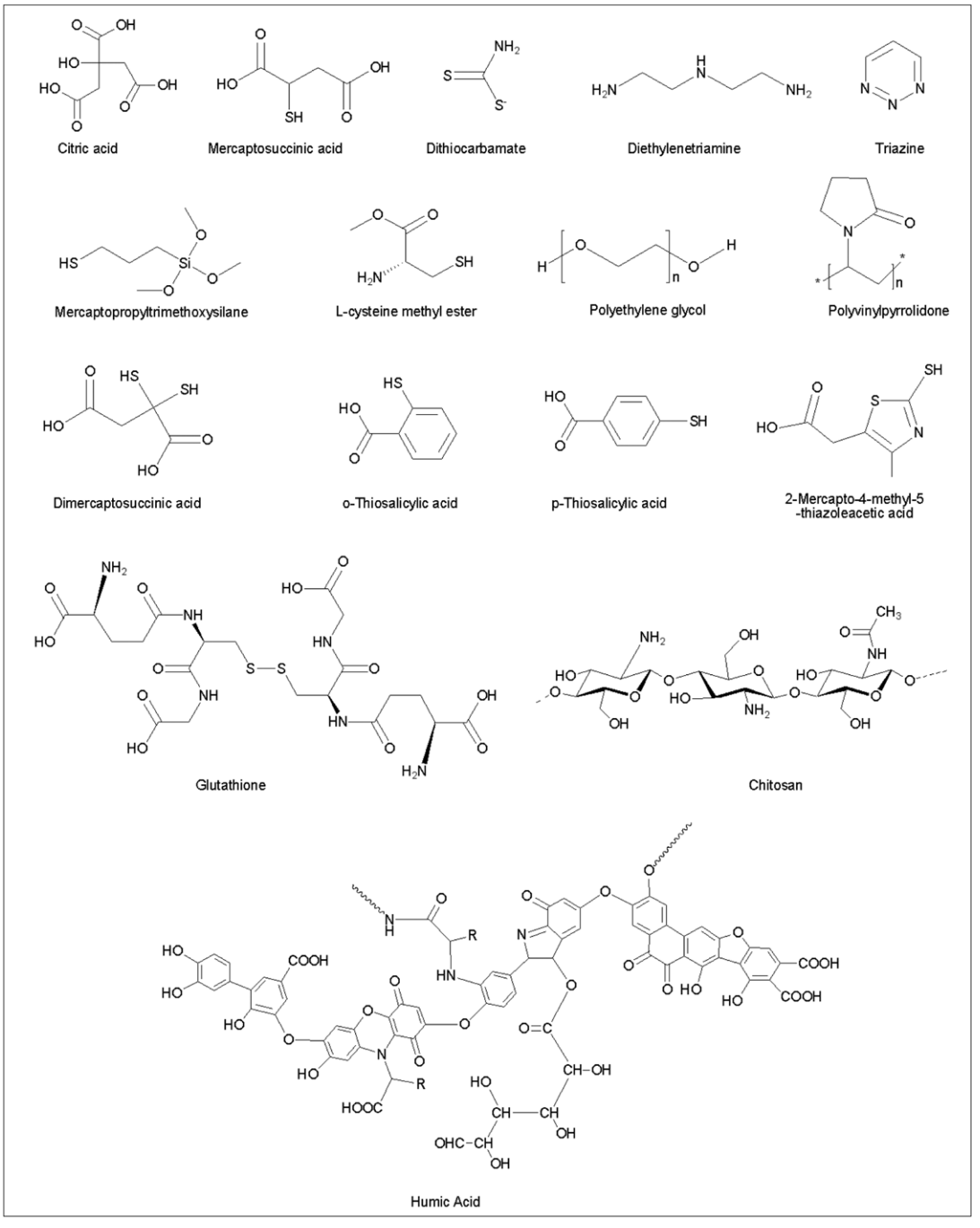

Figure 4. Molecules reported as capping agents for coating nanoparticle surfaces for improving their affinity and selectivity towards mercury adsorption in water.

in o-TSA binds 96% with Pb^{2+}, 90% with Cd^{2+} and 3% with Hg^{2+}; the COOH in p-TSA binds 69% with Pb^{2+}, 65% with Cd^{2+} and 7% with Hg^{2+}. It appeared that the strength of the interaction of COOH in any given molecule follows the order Pb > Cd > Hg. However, when silica nanoparticles were functionalized with these molecules through amide linkage using the COOH groups, the selectivity for Hg adsorption was improved. This was because the COOH group which is selective towards Pb^{2+} and Cd^{2+} was blocked or used in the amidation reaction. The projected SH groups were said to be responsible for Hg^{2+} selective adsorption. Unfortunately, the adsorption of the Hg^{2+} was found to be affected by the steric hindrance of the capping molecules attached to the nanoparticle surface [74].

The fundamental principle that may explain the affinity and selectivity of functionalized nanoadsorbents is Pearson's theory of hard and soft acids and bases—HSAB [73,121]. HSAB theory states that a soft acid would prefer to coordinate and form stronger bonds and more stable complexes

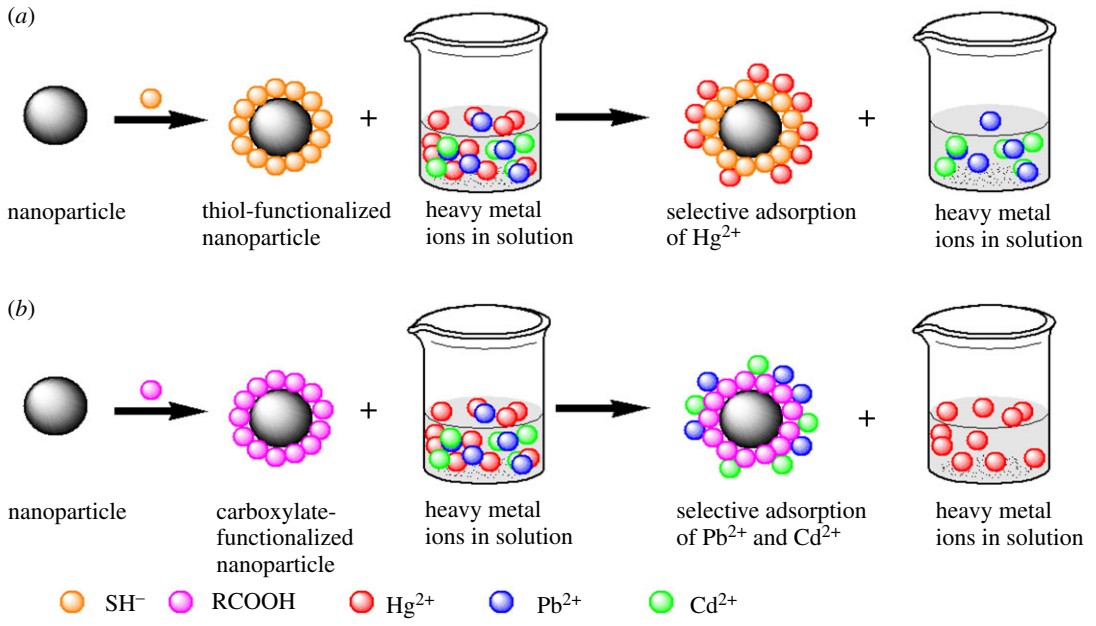

Figure 5. Selective adsorption of heavy metal ions in a solution based on the Pearson's theory of hard and soft acids and bases using inorganic nanoparticle (*a*) thiol functionalized nanoparticle selectively adsorbs Hg^{2+} and (*b*) carboxylate functionalized nanoparticle selectively adsorbs Pb^{2+} and Cd^{2+}.

with soft bases, whereas a hard acid would prefer to coordinate and form stronger bonds and more stable complexes with hard bases [135]. Hard acids are relatively small metal ions that are highly electronegative and have lower polarizabilities, whereas soft acids are relatively large metal ions that are less electronegative and have high polarizabilities [135]. Hg^{2+} and Cd^{2+} are classified as soft acids and usually form stable complexes with soft bases such as SH [135]. COOH and RNH_2 are hard bases and strongly bind with hard acids such as Fe^{3+}, Sn^{2+}, Cr^{3+} and As^{3+} [135]. Pb^{2+}, Ni^{2+}, Fe^{2+}, Cu^{2+} and Zn^{2+} are classified as borderline acids and may prefer to bind with hard or soft bases [135]. Figure 5 shows the binding preferences of COOH and SH groups towards metal ions based on the HSAB theory. The selective adsorptivity of nanoadsorbents towards Hg^{2+} can be enhanced by functionalizing the surface of the nanoparticle with thiol-rich molecules, whereas attaching carboxylic containing molecules will improve adsorption of Pb^{2+}. However, bulky molecules may pose steric restrictions to the approaching cation. The process of nanoparticle surface functionalization can be complicated. Surface functionalization may lead to the reduction of the active surface area of the nanoadsorbents (electronic supplementary material, table S1).

Mehdinia *et al.* [2] observed the decrease of silica nanoparticle surface area by approximately 31% when it was functionalized with thiol groups. However, HA did not reduce the surface area of Fe_3O_4 [83]. It must be stated that the HSAB classification was made based on the equilibrium constants of an acid–base adduct or complex molecule in solution [135]. Fang *et al.* [77] confirms HSAB by attributing the removal efficiency of heavy metals from solution to the solubility products (K_{sp}) of their sulfides, that is, the lower the K_{sp} of the sulfide of the heavy metal, the higher its removal efficiency. However, the effect of K_{sp} on selective adsorption has not been widely studied.

3.3. Regeneration, reusability and stability

The pollutants chemisorb on the surface of the nanoadsorbent, which implies that chemical bonds are formed between the nanoadsorbent and the pollutant. A suitable nanoadsorbent should not have a complicated desorption process. The adsorbed pollutants should be easily desorbed into the solution and the adsorbent re-used. Adsorbents with high recycling or regeneration potential are of greatest interest. Acids, bases, thermal treatment and amalgamation have been used in heavy metals desorption processes. Hg^{2+} was desorbed from a dithio-functionalized magnetic silica nanoparticle by treating with a mixture of 1 M HNO_3 and 2% thiourea, and the recovery efficiency of the Hg^{2+} was greater than 98% after three concurrent uses. The thiourea acted as a chelating agent which complexed with the Hg^{2+} to detach it from the silica nanoparticle surface [2]. Iodine ions also possess

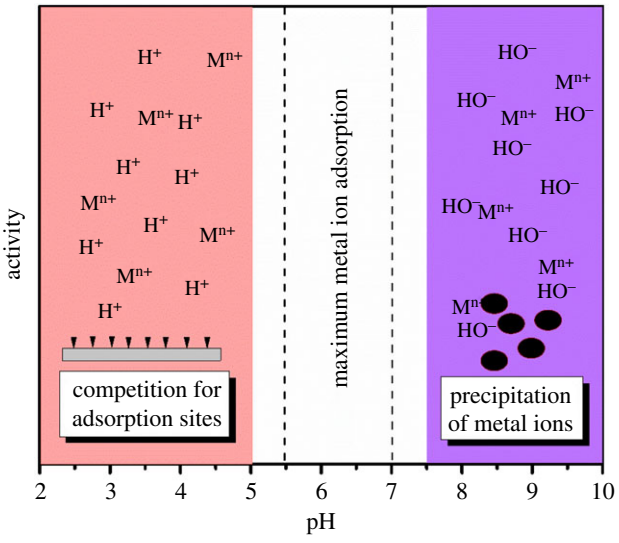

Figure 6. Sketch of a graph showing adsorption characteristics of heavy metal ions on inorganic nanoadsorbents at different pH ranges.

a strong affinity for Hg^{2+} ions, making potassium iodide a suitable recovery agent for detaching Hg^{2+} from adsorbents [134].

The ability of a nanoadsorbent to withstand the desorption processes during regeneration or its resilience in different solvent media determines its stability. Hg^{2+} adsorbed L-cysteine methyl ester dendrimer-capped mixed oxide nanoadsorbent was regenerated using sequential solutions of EDTA, 0.15 M HCl and water, dried at 80°C and re-used more than eight times to achieve adsorption capacity of greater than 97.5% with only a loss of 7% of the dendrimer [71]. Fe_3O_4 nanoparticles are susceptible to air oxidation and tend to aggregate in aqueous solutions [83,111,121]. Coating bare Fe_3O_4 nanoparticles with HAs improves their stability as nanoadsorbent. Liu *et al.* [83] soaked bare Fe_3O_4 and HA-coated Fe_3O_4 nanoparticles in water for 30 days and observed that the bare Fe_3O_4 easily oxidized into brown suspension and lost its magnetization, leaching 0.24 mg l^{-1} of free iron ions in solution, whereas the HA-Fe_3O_4 maintained its magnetization, and only 0.025 mg l^{-1} of free iron ions and 0.16 mg l^{-1} organic carbon were leached into solution. Zhang *et al.* [121] coated Fe_3O_4 with silica which improved its chemical stability, biocompatibility and versatility in surface modification. Similarly, Nasirimoghaddam *et al.* [72] coated Fe_3O_4 with chitosan, a natural polyaminosaccharide, and were able to obtain Hg^{2+} adsorption capacity of 90.58%, whereas the uncoated Fe_3O_4 only removed 41%.

The rate of adsorption of heavy metal ions is dependent on the pH of the solution. At very low pH values, the high concentration of H^+ ions compete with the metal ions for available active sites of the adsorbent material, whereas at high pH values, the OH^- ions tend to precipitate the metal ions, preventing their adsorption. The maximum adsorption of Hg^{2+} has been achieved within pH values of 5–7.5 (figure 6) [8,75,105,134]. Chitosan-bound Fe_3O_4 nanoparticles were able to remove 92.4% of Hg^{2+} ions even at a low pH of 3 [72]. Similarly, 2-mercaptobenzothiazole-coated Fe_3O_4 nanoparticles Hg^{2+} removal efficiency was not significantly affected within a wide pH range of 2.5–11 [78]. The chitosan and 2-mercaptobenzothiazole coatings provided adequate stability to the Fe_3O_4 nanoparticles, thus, making them robust nanoadsorbents. Coating of nanoadsorbents seems a better option for improving the stability in solution and during desorption processes; however, the synthetic process of functionalization of nanoparticle surface remains a major challenge.

In addition, the information on the point of zero charge (pH_{pzc}) of nanoadsorbents is relevant in determining the pH at which the net surface charge is zero, which also ensures the robustness of the adsorbents in different media. The pH_{pzc} indicates the mechanism of adsorption (whether cationic or anionic) and helps in selecting the appropriate pH at which the adsorption process should be carried out in order to minimize precipitation. However, there is little information on pH_{pzc} of various nanoadsorbents in the literature. Electronic supplementary material, table S2 shows the pH_{pzc} of some nanoadsorbents. The surface capping characteristics have a significant effect on the pH_{pzc} of the adsorbent. The pH_{pzc} of bare Fe_3O_4 in 0.01 M NaCl solution was 6.78 and when coated with orange peel powder, reduced to 5.21 [95]. Similarly, Fe_3O_4 nanoparticles capped with sawdust carbon and

L-cysteine had pH_{pzc} values of 4.3–6.1 and 5.7, respectively [89,97]. Capping SiO_2 nanoparticles with APTES ((3-aminopropyl) triethoxysilane) significantly increased the pH_{pzc} from 2.5 to 9.15, indicating improved robustness of the nanoadsorbent in a highly basic environment [88]. However, some material such as ZnO is preferred as nanoadsorbent because it possesses a wide pH_{pzc} value of 8–9 [126].

3.4. Removal of adsorbent from solution

The current trend of nanoadsorbents possesses some level of magnetization which allows them to be easily removed from the solution by applying an external magnet [72]. This makes magnetic nanoadsorbents superior to other non-magnetic adsorbents such as activated charcoal. Fe_3O_4 nanoparticles maintained magnetization at saturation of 79.6 emu g^{-1} even after being coated with HA and only require a low magnetic field gradient for separation from the solution [83]. Non-magnetic inorganic nanoadsorbents can be doped with Fe, Mn and Co ions to impact some level of magnetization; however, very few works have been done using doped nanoparticles as adsorbents.

3.5. The ability of adsorbent to perform other functions

Apart from the adsorption process, some nanoadsorbents have the potential to perform other functions such as amalgamation. Gold forms amalgam with mercury; however, it requires that mercury is in the reduced form Hg^0 before the amalgamation could occur. Not all nanoadsorbents form stable amalgams with the target pollutant. In most instances, Hg^{2+} ions are the predominant form of mercury pollution in water. Ojea-Jiménez *et al*. [104] developed an Au nanoparticle coated with citrate ions which together with its adsorption capabilities was able to reduce Hg^{2+} to Hg^0 which resulted in the formation of amalgam with the Au nanoparticle (Au_3Hg). Thus, the use of very strong and toxic-reducing agents such as $NaBH_4$ was avoided. This observation makes nanoparticles of metals such as silver, copper, tin and aluminium, which form a stable amalgam with Hg attractive and promising nanoadsorbents for sequestration of mercury pollution [6,104]. Iron is a very useful magnetic adsorbent material but does not form a stable amalgam with mercury. However, a more stable amalgam can be obtained by doping the iron nanoparticles such as nZVI with metals that amalgamate with mercury, and this will ensure the effective formation of a more efficient and durable nanoadsorbent for Hg^{2+} removal from water [7].

In addition, magnetite coated with *Lysinibacillus* sp. JLT12 was reported to efficiently reduce Cr(VI) to Cr(III) which is a less toxic and less soluble form of Cr [134]. The kinetics and spectroscopic data showed that the *Lysinibacillus* sp. JLT12 coating was able to remove the passive lepidocrocite and goethite layers of the magnetite to efficiently facilitate the Cr(VI) reduction process [134]. Also, Zhong *et al*. [80] through kinetics and spectroscopic studies attributed the formation of U-O and Mn-O-U bonds to the oxygen-containing groups in δ-MnO_2@COF nanocomposite, which resulted in ultra-fast removal of UO_2^{2+} radionuclide from water.

These extra abilities of inorganic nanoadsorbents demonstrate that efficient adsorbents can be designed and hold promise for efficient environmental remediation processes.

4. Environmental application

Hofacker *et al*. [135] in soil microcosm experiments demonstrated the potential application of inorganic nanoparticles in environmental remediation processes. The researchers set out to study mercury mobilization in flooded soil by incorporation into metallic copper and metal sulfide nanoparticles. The soil studied were topsoil samples obtained from the contaminated floodplain of the River Mulde in Germany, which were polluted with 0.91–1.26 mg kg^{-1} Hg and 160–279 mg kg^{-1} Cu. This level of pollution was 10 times the average content of European floodplain soils. Soil flooding experiments were carried out with air-dried soil (amended with lactate, which promotes activities of soil microorganisms including Fe and sulfate reducers) that was flooded with synthetic river water (containing 0.6 mM NaCl, 0.6 mM $CaSO_4$ and 0.3 mM $Mg(NO_3)_2$) and incubated at different periods and temperatures. Soil pore water samples were withdrawn, acidified, filtered and analysed for Hg, Cu, Fe, Mn and metal sulfides.

The study showed that the formation of Hg-Cu amalgam nanoparticles may be a common process induced by soil flooding under limited sulfate availability. However, during sulfate reduction, Hg was effectively incorporated into nanoparticulate metal sulfides. Figure 7 shows STEM-HAADF images

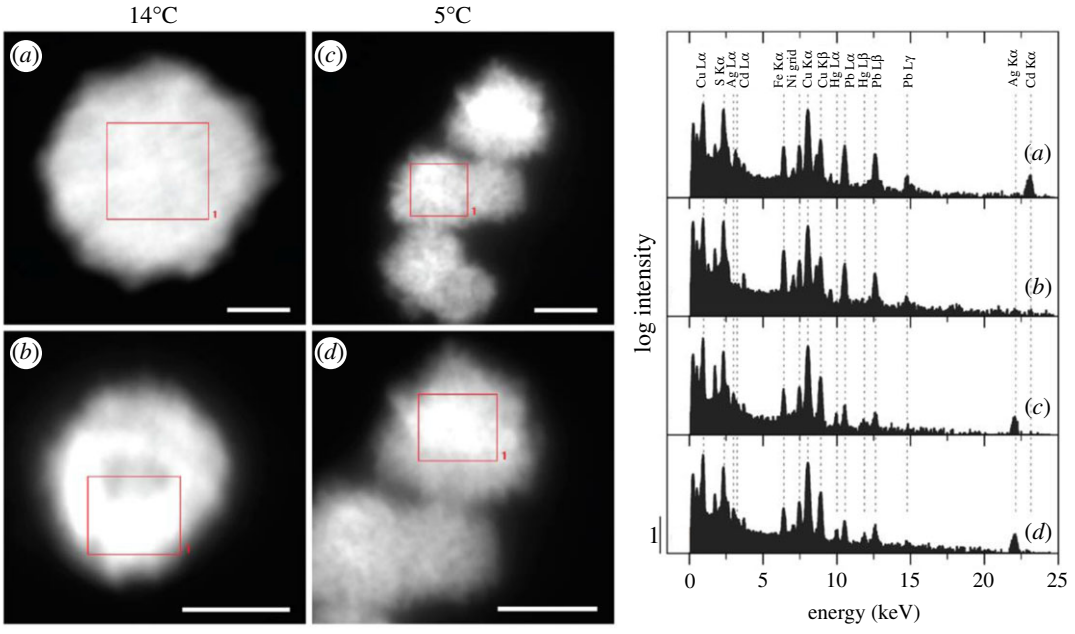

Figure 7. STEM-HAADF images and EDX spectra of metal sulfide nanoparticles formed after 12 days of flooding at 14°C (*a*,*b*) and after 33 days of flooding at 5°C (*c*,*d*). Scale bars represent 50 nm. EDX spectra were recorded on areas marked by red rectangles. Reprinted with permission from Hofacker *et al*. [135]. Copyright (2021) American Chemical Society.

and EDX spectra of metal sulfide nanoparticles formed after 12 days and 33 days of flooding at 14°C and 5°C, respectively. The tendency for different metals to precipitate with a limited amount of sulfide during soil flooding depends on the thermodynamic stability of the respective metal sulfides (Hg > Ag > Cu > Cd ~ Pb > Zn > Fe). Also, coprecipitated Fe or Zn may be exchanged for Hg, Ag, Cu, Cd or Pb due to the lower stability of Fe and Zn monosulfides. Thus, based on the extremely high thermodynamic stability of HgS, higher soil Hg/Cu ratios are expected to favour the formation of pure HgS over mixed metal sulfide formation. The study showed that Hg incorporation into metallic Cu and metal sulfide nanoparticles can cause substantial colloidal Hg mobilization into the pore water. When exposed to oxygen, metal sulfide nanoparticles were found to be stable against oxidation in oxygenated water for up to several weeks. The formation of HgS was suggested to probably affect the extent of Hg methylation and volatilization which are the most toxic and dangerous aspects of Hg pollution.

Although Hofacker *et al*.'s [135] work demonstrates how soil floods induce the formation of inorganic nanoparticles depending on the soil's mineral composition, it does not show in real time how they could be applied to environmental remediation. Their work, however, suggests potential removal of Hg from aqueous solution using metal Cu and metal (Fe and Zn) sulfide nanoparticles through the formation of Hg-Cu amalgam and highly thermodynamic stable HgS nanoparticles precipitates, which can be filtered out of solution.

5. Conclusion

It has been established that inorganic nanoadsorbent materials address the problem of environmental pollution. Heavy metal contamination levels of over 100 mg l^{-1} have been removed, attaining a very high adsorption capacity of less than or equal to 3449 mg g^{-1} with inorganic nanoadsorbents with less than 2 g l^{-1} adsorbent dosage. Although inorganic nanoadsorbents hold much promise in environmental remediation, there are very important bottlenecks that have to be addressed to harness their full potential. Some of the bottlenecks are:

(i) Metal nanoparticles such as Ag and Au are generally expensive for adsorption purposes. Thus, cheaper materials or earth-abundant metals would be more useful.
(ii) n-ZVI nanoparticles are very efficient but they are extremely reactive and may be unstable. More research efforts would be required to develop the core–shell counterparts to improve the stability.

(iii) Iron oxides nanoparticles have been widely used because they are magnetic and facilitate easy separation from solution; however, their heavy metal adsorption capacities are lower compared with CuO, ZnO, SnO and MgO nanoparticles which are not magnetic. Thus, doping nanoparticles with magnetic materials becomes an attractive strategy to improve the separability property of nanoadsorbents.

(iv) Metal sulfides nanoparticles have a higher affinity for heavy metals compared with metal oxides; however, they are less studied for remediation processes.

(v) It is worth noting that the control of selectivity in heavy metal adsorption has been associated with Pearson's theory of hard and soft acids and bases, but unfortunately, there is very little information to clearly explain the selectivity concept. The key responsible principle has been associated with the complexation of the heavy metals by functional groups on the inorganic nanoadsorbents surfaces. Although ligands attached to surfaces of nanoparticles improve the selectivity of nanoadsorbents towards target heavy metal, the process of nanoparticle surface functionalization can be very challenging and requires considerable research effort to improve on the qualities of inorganic nanoadsorbents.

In the design of good quality inorganic adsorbent, the nanoparticle synthesis method, selectivity, stability, regeneration and reusability, and adsorbent separation from solution are critical concerns. It is intended in the future that stable nanoadsorbents that are selective to specific pollutants, easy to synthesize (in an environmentally friendly manner) and separated from the solution, and also can perform other important functions are developed.

Ethics. This statement is not relevant to this work.

Data accessibility. Additional tables showing the BET surface area and point of zero charge of some inorganic nanoadsorbents have been provided in the electronic supplementary material.

Authors' contributions. M.B.M. designed, obtained literature and drafted the manuscript. D.J.L., N.O.B. and J.A.M.A. revised the manuscript critically for important intellectual content.

Competing interests. The authors declare no competing interests.

Funding. This work was funded by Leverhulme-Royal Society Africa Award-Postdoctoral Fellowship grant (grant no. LAF\R1\180018)

Acknowledgements. J.A.M.A., D.J.L. and M.B.M. wish to acknowledge the Leverhulme-Royal Society Africa Award-Postdoctoral Fellowship grant no. (LAF\R1\180018) for providing financial support for this project. The DFID-Royal Society Africa Capacity Building Initiative (ACBI) is acknowledged for support to J.A.M.A. and D.J.L. The Department of Chemistry, Kwame Nkrumah University of Science and Technology, Kumasi, is acknowledged for hosting the fellowship.

References

1. WHO 2011 *Guidelines for drinking-water quality*, 4th edn. World Health Organization.
2. Mehdinia A, Akbari M, Kayyal TB, Azad M. 2014 High-efficient mercury removal from environmental water samples using di-thio grafted on magnetic mesoporous silica nanoparticles. *Env. Sci. Pollut. Res.* **22**, 2155–2165. (doi:10.1007/s11356-014-3430-6)
3. Armah FA, Luginaah I, Odoi J. 2013 Artisanal small-scale mining and mercury pollution in Ghana: a critical examination of a messy minerals and gold mining policy. *J. Env. Stud. Sci.* **3**, 381–390. (doi:10.1007/s13412-013-0147-7)
4. Appleton JD, Williams TM, Breward N, Apostol A, Miguel J. 1999 Mercury contamination associated with artisanal gold mining on the island of Mindanao, the Philippines. *Sci. Total Environ.* **228**, 95–109. (doi:10.1016/S0048-9697(99)00016-9)
5. García O, Veiga MM, Cordy P, Suescún OE, Martin J, Roeser M. 2014 Artisanal gold mining in Antioquia, Colombia: a successful case of mercury reduction. *J. Clean Prod.* **90**, 244–252. (doi:10.1016/j.jclepro.2014.11.032)
6. Kamarudin KSN, Mohamad MF. 2010 Synthesis of gold (Au) nanoparticles for mercury adsorption. *Am. J. Appl. Sci.* **7**, 835–839. (doi:10.3844/ajassp.2010.835.839)
7. Yan W, Herzing AA, Kiely CJ, Zhang W-X. 2010 Nanoscale zero-valent iron (nZVI): aspects of the core-shell structure and reactions with inorganic species in water. *J. Contam. Hydrol.* **118**, 96–104. (doi:10.1016/j.jconhyd.2010.09.003)
8. Dixit A, Mishra PK, Alam MS. 2017 Titania nanofibers: a potential adsorbent for mercury and lead uptake. *Int. J. Chem. Eng. Appl.* **8**, 75–81. (doi:10.18178/ijcea.2017.8.1.633)
9. Solis KL, Nam GU, Hong Y. 2016 Effectiveness of gold nanoparticle-coated silica in the removal of inorganic mercury in aqueous systems: equilibrium and kinetic studies. *Environ. Eng. Res.* **21**, 99–107. (doi:10.4491/eer.2015.126)
10. Kessler R. 2013 The Minamata convention on mercury: a first step toward protecting future generations. *Environ. Health Perspect.* **121**, 304–309. (doi:10.1289/ehp.121-a304)
11. CSEM. 2017 Lead toxicity. *Agency Toxic Subst. Dis. Regist.* 1–24.
12. CSEM. 2008 Cadmium toxicity. *Agency Toxic Subst. Dis. Regist.* 1–63.
13. Akoto O, Bruce TN, Darko G. 2008 Heavy metals pollution profiles in streams serving the Owabi reservoir. *Afr. J. Environ. Sci. Technol.* **2**, 354–359.
14. Boamponsem LK, Adam JI, Dampare SB, Nyarko BJB, Essumang DK. 2010 Assessment of atmospheric heavy metal deposition in the Tarkwa gold mining area of Ghana using epiphytic lichens. *Nucl. Inst. Methods Phys. Res. B* **268**, 1492–1501. (doi:10.1016/j.nimb.2010.01.007)
15. Donkor AK, Bonzongo JCJ, Nartey VK, Adotey DK. 2005 Heavy metals in sediments of the gold mining impacted Pra River basin, Ghana, West Africa. *Soil Sediment Contam.* **14**, 479–503. (doi:10.1080/15320380500263675)
16. Gbogbo F, Otoo SD, Huago RQ, Asomaning O. 2016 High levels of mercury in wetland resources from three river basins in Ghana: a concern for public health. *Environ. Sci. Pollut. Res.* **24**, 5619–5627. (doi:10.1007/s11356-016-8309-2)

17. Laar C, Anim A, Osei J, Bimi L. 2011 Effect of anthropogenic activities on an ecologically important wetland in Ghana. *J. Biodivers. Environ. Sci.* **1**, 9–21.
18. Tay C, Momade F. 2006 Trace metal contamination in water from abandoned mining and non-mining areas in the northern parts of the Ashanti Gold Belt, Ghana. *West Afr. J. Appl. Ecol.* **10**, 1–16. (doi:10.4314/wajae.v10i1.45714)
19. Attua EM, Annan ST, Nyame F. 2014 Water quality analysis of rivers used as drinking sources in artisanal gold mining communities of the Akyem-Abuakwa area: a multivariate statistical approach. *Ghana J. Geogr.* **6**, 24–41.
20. Adjorlolo-Gasokpoh A, Golow AA, Kambo-Dorsa J. 2012 Mercury in the surface soil and cassava, *Manihot esculenta* (flesh, leaves and peel) near goldmines at Bogoso and Prestea, Ghana. *Bull. Environ. Contam. Toxicol.* **89**, 1106–1110. (doi:10.1007/s00128-012-0849-7)
21. Affum AO, Dede SO, Nyarko BJB, Acquaah SO, Kwaansa-Ansah EE, Darko G, Dickson A, Affum EA, Fianko JR. 2016 Influence of small-scale gold mining and toxic element concentrations in Bonsa River, Ghana: a potential risk to water quality and public health. *Environ. Earth Sci.* **75**, 1–17. (doi:10.1007/s12665-015-5000-8)
22. Dankwa HR, Biney CA, DeGraft-Johnson KAA. 2005 Impact of mining operations on the ecology of River Offin in Ghana. *West Afr. J. Appl. Ecol.* **7**, 19–30. (doi:10.4314/wajae.v7i1.45638)
23. Donkor AK, Nartey VK, Bonzongo JC, Adotey DK. 2006 Artisanal mining of gold with mercury in Ghana. *West Afr. J. Appl. Ecol.* **9**, 1–8. (doi:10.4314/wajae.v9i1.45666)
24. Adjei-Boateng D, Obirikorang KA, Amisah S, Madkour HA, Otchere FA. 2011 Relationship between gonad maturation and heavy metal accumulation in the clam, *Galatea paradoxa* (Born 1778) from the Volta Estuary, Ghana. *Bull Env. Contam. Toxicol.* **87**, 626–632. (doi:10.1007/s00128-011-0417-6)
25. Oppong SOB, Voegborlo RB, Agorku SE, Adimado AA. 2010 Total mercury in fish, sediments and soil from the River Pra Basin, Southwestern Ghana. *Bull. Environ. Contam. Toxicol.* **85**, 324–329. (doi:10.1007/s00128-010-0059-0)
26. Asare-Donkor NK, Adimado AA. 2016 Influence of mining related activities on levels of mercury in water, sediment and fish from the Ankobra and Tano River basins in South Western Ghana. *Environ. Syst. Res.* **5**, 1–11. (doi:10.1186/s40068-016-0055-4)
27. Ahiamadjie H, Serfor-Armah Y, Tandoh JB, Gyampo O, Ofosu FG, Dampare SB, Adotey DK, Nyarko BJB. 2011 Evaluation of trace elements contents in staple foodstuffs from the gold mining areas in southwestern part of Ghana using neutron activation analysis. *J. Radioanal. Nucl. Chem.* **288**, 653–661. (doi:10.1007/s10967-011-0979-0)
28. Dorleku MK, Nukpezah D, Carboo D. 2018 Effects of small-scale gold mining on heavy metal levels in groundwater in the Lower Pra Basin of Ghana. *Appl. Water Sci.* **8**, 1–11. (doi:10.1007/s13201-018-0773-z)
29. Oduro WO, Bayitse R, Carboo D, Hodgson I. 2012 Assessment of dissolved mercury in surface water along the lower basin of the River Pra in Ghana. *Int. J. Sci. Technol.* **2**, 228–235.
30. Nartey VK, Klake RK, Doamekpor LK. 2012 Speciation of mercury in mine waste: case study of abandoned and active gold mine sites at the Bibiani–Anwiaso–Bekwai area of South Western Ghana. *Env. Monit. Assess.* **184**, 7623–7634. (doi:10.1007/s10661-012-2523-2)
31. Hayford EK, Amin A, Osae EK, Kutu J. 2008 Impact of gold mining on soil and some staple foods collected from selected mining communities in and around Tarkwa-Prestea area. *West Afr. J. Appl. Ecol.* **14**, 1–12. (doi:10.4314/wajae.v14i1.44708)
32. Akabzaa TM, Jamieson HE, Jorgenson N, Nyame K. 2009 The combined impact of mine drainage in the Ankobra River Basin, SW Ghana. *Mine Water Env.* **28**, 50–64. (doi:10.1007/s10230-008-0057-1)
33. Kortatsi BK. 2007 Hydrochemical framework of groundwater in the Ankobra Basin, Ghana. *Aquat. Geochem.* **13**, 41–74. (doi:10.1007/s10498-006-9006-4)
34. Dwumah-Ankoana S. 2008 Studies on levels of mercury, cadmium and zinc in fish and sediments from River Offin in Ghana. MSc thesis, Department of Chemistry, Kwame Nkrumah University of Science and Technology, Kumasi, Ghana.
35. Azanu D, Voegborlo RB. 2013 Sorption of inorganic mercury on soils from Ankobra basin in the south-western part of Ghana. *J. Sci. Technol.* **33**, 1–15. (doi:10.4314/just.v33i3.1)
36. Serfor-Armah Y, Adotey DK, Adomako D, Akaho EHK, Nyarko BJB. 2004 The impact of small-scale mining activities on the levels of mercury in the environment: the case of Prestea and its environs. *J. Radioanal. Nucl. Chem.* **262**, 685–690. (doi:10.1007/s10967-005-0493-3)
37. Nansen F. 2009 Marine environmental survey of bottom sediments in Ghana. In *FAO Project:GCP/INT/003/NOR*, 1–50.
38. Darko G, Dodd M, Nkansah MA, Ansah E, Aduse-Poku Y. 2017 Distribution and bioaccessibility of metals in urban soils of Kumasi. *Ghana. Env. Monit. Assess.* **189**, 1–13. (doi:10.1007/s10661-017-5972-9)
39. Rajaee M, Long RN, Renne EP, Basu N. 2015 Mercury exposure assessment and spatial distribution in a Ghanaian small-scale gold mining community. *Int. J. Environ. Res. Public Heal.* **12**, 10 755–10 782. (doi:10.3390/ijerph120910755)
40. Kodom K, Preko K, Boamah D. 2012 X-ray fluorescence (XRF) analysis of soil heavy metal pollution from an industrial area in Kumasi, Ghana. *Soil Sediment Contam.* **21**, 1006–1021. (doi:10.1080/15320383.2012.712073)
41. Klake RK, Nartey VK, Doamekpor LK, Edor KA. 2012 Correlation between heavy metals in fish and sediment in Sakumo and Kpeshie Lagoons, Ghana. *J. Environ. Prot (Irvine, Calif).* **3**, 1070–1077. (doi:10.4236/jep.2012.39125)
42. Obiri S. 2007 Determination of heavy metals in water from boreholes in Dumasi in the Wassa West District of Western Region of Republic of Ghana. *Env. Monit. Assess.* **130**, 455–463. (doi:10.1007/s10661-006-9435-y)
43. Kodom K, Wiafe-Akenten J, Boamah D. 2010 *Soil heavy metal pollution along Subin river in Kumasi, Ghana; using X-ray fluorescence (XRF) analysis*. In *CP1221, X-Ray Optic and Microanalysis, Proc. of the 20th Int. Congress*, pp. 101–108.
44. Boateng TK, Opoku F, Acquaah SO, Akoto O. 2015 Pollution evaluation, sources and risk assessment of heavy metals in hand-dug wells from Ejisu-Juaben Municipality, Ghana. *Environ. Syst. Res.* **4**, 1–12. (doi:10.1186/s40068-015-0045-y)
45. Adokoh CK, Essumang DK. 2011 Statistical evaluation of environmental contamination, distribution and source assessment of heavy metals (aluminum, arsenic, cadmium, and mercury) in some lagoons and an estuary along the coastal belt of Ghana. *Arch. Env. Contam. Toxicol.* **61**, 369–400. (doi:10.1007/s00244-011-9643-5)
46. Armah FA, Gyeabour EK. 2013 Health risks to children and adults residing in riverine environments where surficial sediments contain metals generated by active gold mining in Ghana. *Toxicol. Res.* **29**, 69–79. (doi:10.5487/TR.2013.29.1.069)
47. Obiri S, Yeboah PO, Osae S, Adu-Kumi S, Cobbina S, Armah F, Ason B, Antwi E, Quansah R. 2016 Human health risk assessment of artisanal miners exposed to toxic chemicals in water and sediments in the Presteahuni Valley district of Ghana. *Int. J. Environ. Res. Public Health* **13**, 139. (doi:10.3390/ijerph13010139)
48. Eze PN, Udeigwe TK, Stietiya MH. 2010 Distribution and potential source evaluation of heavy metals in prominent soils of Accra Plains, Ghana. *Geoderma* **156**, 357–362. (doi:10.1016/j.geoderma.2010.02.032)
49. Fosu-mensah BY, Addae E, Yirenya-tawiah D, Nyame F. 2017 Heavy metals concentration and distribution in soils and vegetation at Korle Lagoon area in Accra, Ghana. *Cogent Environ. Sci.* **3**, 1–14. (doi:10.1080/23311843.2017.1405887)
50. Bempah CK, Ewusi A. 2016 Heavy metals contamination and human health risk assessment around Obuasi gold mine in Ghana. *Env. Monit. Assess.* **188**, 1–13. (doi:10.1007/s10661-016-5241-3)
51. Hogarh JN, Adu-Gyamfi E, Nukpezah D, Akoto O, Kumi SA. 2016 Contamination from mercury and other heavy metals in a mining district in Ghana: discerning recent trends from sediment core analysis. *Environ. Syst. Res.* **5**, 1–9. (doi:10.1186/s40068-016-0067-0)
52. Zango MS, Anim-gyampo M, Ampadu B. 2013 Health risks of heavy metals in selected food crops cultivated in small-scale gold-mining areas in Wassa-Amenfi-West District of Ghana. *J. Nat. Sci. Res.* **3**, 96–105.
53. Bortey-Sam N, Nakayama SMM, Akoto O, Ikenaka Y, Baidoo E, Mizukawa H, Ishizuka M. 2015 Ecological risk of heavy metals and a metalloid in agricultural soils in Tarkwa, Ghana. *Int. J. Environ. Res. Public Heal.* **12**, 11 448–11 465. (doi:10.3390/ijerph120911448)

54. Cobbina SJ, Duwiejuah AB, Quansah R, Obiri S. 2015 Comparative assessment of heavy metals in drinking water sources in two small-scale mining communities in northern Ghana. *Int. J. Environ. Res. Public Heal.* **064**, 10 620–10 634. (doi:10.3390/ijerph120910620)
55. Bhattacharya P *et al.* 2012 Hydrogeochemical study on the contamination of water resources in a part of Tarkwa mining area, western Ghana. *J. Afr. Earth Sci.* **66–67**, 72–84. (doi:10.1016/j.jafrearsci.2012.03.005)
56. Vowotor MK *et al.* 2014 An assessment of heavy metal pollution in sediments of a tropical lagoon: a case study of the Benya Lagoon, Komenda Edina Eguafo Abrem Municipality (KEEA) — Ghana. *J. Heal Pollut.* **4**, 26–39. (doi:10.5696/2156-9614-4-6.26)
57. Acheampong F, Akenten JW, Imoro R, Agbesie HR, Abaye D. 2016 Evaluation of heavy metal pollution in the Suame Industrial Area, Kumasi, Ghana. *J. Heal. Pollut.* **6**, 56–63. (doi:10.5696/2156-9614-6-10.56)
58. Kpan JDA, Opoku BK, Gloria A. 2014 Heavy metal pollution in soil and water in some selected towns in Dunkwa-on-Offin District in the Central Region of Ghana as a result of small scale gold mining. *J. Agric. Chem. Environ.* **3**, 40–47. (doi:10.4236/jacen.2014.32006)
59. Sadick A, Amfo-Otu R, Acquah SJ, Nketia KA, Asamoah E, Adjei EO. 2015 Assessment of heavy metal contamination in soils around auto mechanic worshop clusters in central agricultural station, Kumasi-Ghana. *Appl. Res. J.* **1**, 12–19.
60. Antwi-Agyei P, Hogarh JN, Foli G. 2009 Trace elements contamination of soils around gold mine tailings dams at Obuasi, Ghana. *Afr. J. Environ. Sci. Technol.* **3**, 353–359. (doi:10.5251/ajsms.2010.1.1.1.12)
61. Tay CK, Asmah R, Biney CA. 2009 Trace metal levels in water and sediment from the Sakumo II and Muni Lagoons, Ghana. *West Afr. J. Appl. Ecol.* **16**, 75–94. (doi:10.4314/wajae.v16i1.55870)
62. Afum BO, Owusu CK. 2016 Heavy metal pollution in the Birim River of Ghana. *Int. J. Environ. Monit. Anal.* **4**, 65–74. (doi:10.11648/j.ijema.20160403.11)
63. Adjei-Kyereme Y, Donkor AK, Golow AA, Yeboah PO, Pwamang J. 2015 Mercury concentrations in water and sediments in rivers impacted by artisanal gold mining in the Asutifi District, Ghana. *Res. J. Chem. Environ. Sci.* **3**, 40–48.
64. Bentum JK, Anang M, Boadu KO, Koranteng-Addo AE. 2011 Assessment of heavy metals pollution of sediments from Fosu lagoon in Ghana. *Bull. Chem. Soc. Ethiop.* **25**, 191–196. (doi:10.4314/bcse.v25i2.65869)
65. Fianko JR, Osae S, Adomako D, Adotey DK. 2007 Assessment of heavy metal pollution of the Ture estuary in the Central Region of Ghana. *Env. Monit. Assess.* **131**, 467–473. (doi:10.1007/s10661-006-9492-2)
66. Obiri-Danso K, Adjei B, Stanley KN, Jones K. 2009 Microbiological quality and metal levels in wells and boreholes water in some peri-urban communities in Kumasi, Ghana. *Afr. J. Environ. Sci. Technol.* **3**, 59–66. (doi:10.5897/AJEST08.126)
67. Akabzaa TM, Yidana SM. 2011 Evaluation of sources and options for possible clean up of anthropogenic mercury contamination in the Ankobra River Basin in South Western Ghana. *J. Environ. Prot. (Irvine, Calif).* **02**, 1295–1302. (doi:10.4236/jep.2011.210149)
68. Agyarko K, Dartey E, Kuffour R, Sarkodie P. 2014 Assessment of trace elements levels in sediment and water in some artisanal and small-scale mining (ASM) localities in Ghana. *Curr. World Environ. J.* **9**, 7–16. (doi:10.12944/cwe.9.1.02)
69. Babut M, Sekyi R, Rambaud A, Potin-Gautier M, Tellier S, Bannerman W, Beinhoff C. 2003 Improving the environmental management of smallscale goldmining in Ghana: a case study of Dumasi. *J. Clean Prod.* **11**, 215–221. (doi:10.1016/S0959-6526(02)00042-2)
70. Bannerman W, Potin-Gautier M, Amouroux D, Tellier S, Rambaud A, Babut M, Adimado A, Beinhoff C. 2003 Mercury and arsenic in the gold mining regions of the Ankobra River basin in Ghana. *J. Phys. IV Fr.* **107**, 107–110. (doi:10.1051/jp4:20030255)
71. Arshadi M, Firouzabadi H, Abbaspourrad A. 2017 Adsorption of mercury ions from wastewater by a hyperbranched and multi-functionalized dendrimer modified mixed-oxides nanoparticles. *J. Colloid Interface Sci.* **505**, 293–306. (doi:10.1016/j.jcis.2017.05.052)
72. Nasirimoghaddam S, Zeinali S, Sabbaghi S. 2015 Chitosan coated magnetic nanoparticles as nano-adsorbent for efficient removal of mercury contents from industrial aqueous and oily samples. *J. Ind. Eng. Chem.* **27**, 79–87. (doi:10.1016/j.jiec.2014.12.020)
73. Košak A, Lobnik A, Bauman M. 2015 Adsorption of mercury(II), lead(II), cadmium(II) and zinc(II) from aqueous solutions using mercapto-modified silica particles. *Int. J. Appl. Ceram. Technol.* **12**, 461–472. (doi:10.1111/ijac.12180)
74. Hamid AAA, Tripp CP, Bruce AE, Bruce MRM. 2011 Application of structural analogs of dimercaptosuccinic acid-functionalized silica nanoparticles (DMSA-[silica]) to adsorption of mercury, cadmium and lead. *Res. Chem. Intermed.* **37**, 791–810. (doi:10.1007/s11164-011-0317-8)
75. Rahbar N, Jahangiri A, Boumi S, Khodayar MJ. 2014 Mercury removal from aqueous solutions with chitosan-coated magnetite nanoparticles optimized using the Box-Behnken design. *Jundishapur J. Nat. Pharm. Prod.* **9**, 2. (doi:10.17795/jjnpp-15913)
76. Özsin G, Kılıç M, Apaydın E, Ayşe V, Pütün E. 2019 Chemically activated carbon production from agricultural waste of chickpea and its application for heavy metal adsorption: equilibrium, kinetic, and thermodynamic studies. *Appl. Water Sci.* **9**, 1–14. (doi:10.1007/s13201-019-0942-8)
77. Fang L, Li L, Qu Z, Xu H, Xu J, Yan N. 2018 A novel method for the sequential removal and separation of multiple heavy metals from wastewater. *J. Hazard. Mater.* **342**, 617–624. (doi:10.1016/j.jhazmat.2017.08.072)
78. Parham H, Zargar B, Shiralipour R. 2012 Fast and efficient removal of mercury from water samples using magnetic iron oxide nanoparticles modified with 2-mercaptobenzothiazole. *J. Hazard. Mater.* **205–206**, 94–100. (doi:10.1016/j.jhazmat.2011.12.026)
79. Sarkar ZK, Sarkar VK. 2018 Removal of mercury (II) from wastewater by magnetic solid phase extraction with polyethylene glycol (PEG)-coated Fe_3O_4 nanoparticles. *Int. J. Nanosci. Nanotechnol.* **14**, 65–70.
80. Zhong X, Lu Z, Liang W, Guo X, Hu B. 2020 Fabrication of 3D hierarchical flower-like sigma-MnO_2@COF nanocomposites for the efficient and ultra-fast removal of UO_2^{2+} ion from aqueous solution. *Environ. Sci. Nano.* **7**, 3303–3317. (doi:10.1039/D0EN00793E)
81. Liu Y *et al.* 2021 Zeolitic imidazolate framework-based nanomaterials for the capture of heavy metal ions and radionuclides: a review. *Chem. Eng. J.* **406**, 127139. (doi:10.1016/j.cej.2020.127139)
82. Ray PZ, Shipley HJ. 2015 Inorganic nano-adsorbents for the removal of heavy metals and arsenic: a review. *RSC Adv.* **5**, 29 885–29 907. (doi:10.1039/c5ra02714d)
83. Liu JF, Zhao ZS, Jiang GB. 2008 Coating Fe_3O_4 magnetic nanoparticles with humic acid for high efficient removal of heavy metals in water. *Environ. Sci. Technol.* **42**, 6949–6954. (doi:10.1021/es800924c)
84. Kyzas GZ, Deliyanni EA. 2013 Mercury(II) removal with modified magnetic chitosan adsorbents. *Molecules* **18**, 6193–6214. (doi:10.3390/molecules18066193)
85. Fakhri A. 2014 Investigation of mercury (II) adsorption from aqueous solution onto copper oxide nanoparticles: optimization using response surface methodology. *Process Saf. Environ. Prot.* **93**, 201–205. (doi:10.1016/j.psep.2014.06.003)
86. Gong Y, Liu Y, Xiong Z, Zhao D. 2014 Immobilization of mercury by carboxymethyl cellulose stabilized iron sulfide nanoparticles: reaction mechanisms and effect of stabilizer and water chemistry. *Envrion. Sci. Technol.* **48**, 3986–3994. (doi:10.1021/es404418a)
87. Rajput S, Singh LP, Pittman Jr CU, Mohan D. 2016 Lead (Pb^{2+}) and copper (Cu^{2+}) remediation from water using superparamagnetic maghemite (γ-Fe_2O_3) nanoparticles synthesized by flame spray pyrolysis (FSP). *J. Colloid Interface Sci.* **492**, 176–190. (doi:10.1016/j.jcis.2016.11.095)
88. Guivar JAR, Sadrollahi E, Menzel D, Fernandes EG, López EO, Torres MM, Arsuaga JM, Arencibia A, Litterst FJ. 2017 Magnetic, structural and surface properties of functionalized maghemite nanoparticles for copper and lead adsorption. *RSC Adv.* **7**, 28 763–28 779. (doi:10.1039/c7ra02750h)
89. Bagbi Y, Sarswat A, Mohan D, Pandey A, Solanki PR. 2017 Lead and chromium adsorption from water using L-cysteine functionalized magnetite (Fe_3O_4) nanoparticles. *Sci. Rep.* **7**, 1–15. (doi:10.1038/s41598-017-03380-x)
90. Arce VB *et al.* 2015 EXAFS and DFT study of the cadmium and lead adsorption on modified silica nanoparticles. *Spectrochim. Acta* **151**, 156–163. (doi:10.1016/j.saa.2015.06.093)
91. Salam MA. 2012 Coating carbon nanotubes with crystalline manganese dioxide nanoparticles and their application for lead ions removal from

model and real water. *Colloids Surf. A Physicochem. Eng. Asp.* **419**, 69–79. (doi:10.1016/j.colsurfa.2012.11.06)

92. Cao C, Qu J, Wei F, Liu H, Song W. 2012 Superb adsorption capacity and mechanism of flowerlike magnesium oxide nanostructures for lead and cadmium ions. *Appl. Mater. Interfaces* **4**, 4283–4287. (doi:10.1021/am300972z)
93. Kumar KY, Raj TNV, Archana S, Prasad SBB, Olivera S, Muralidhara HB. 2016 SnO_2 nanoparticles as effective adsorbents for the removal of cadmium and lead from aqueous solution: adsorption mechanism and kinetic studies. *J. Water Process Eng.* **13**, 44–52. (doi:10.1016/j.jwpe.2016.07.007)
94. Boparai HK, Joseph M, Carroll DMO. 2011 Kinetics and thermodynamics of cadmium ion removal by adsorption onto nano zerovalent iron particles. *J. Hazard. Mater.* **186**, 458–465. (doi:10.1016/j.jhazmat.2010.11.029)
95. Gupta VK, Nayak A. 2012 Cadmium removal and recovery from aqueous solutions by novel adsorbents prepared from orange peel and Fe_2O_3 nanoparticles. *Chem. Eng. J.* **180**, 81–90. (doi:10.1016/j.cej.2011.11.006)
96. Kataria N, Garg VK. 2018 Green synthesis of Fe_3O_4 nanoparticles loaded sawdust carbon for cadmium (II) removal from water: regeneration and mechanism. *Chemosphere* **208**, 818–828. (doi:10.1016/j.chemosphere.2018.06.022)
97. Shah J, Jan MR, Khan M, Amir S. 2015 Removal and recovery of cadmium from aqueous solutions using magnetic nanoparticle-modified sawdust: kinetics and adsorption isotherm studies. *Desalin Water Treat.* **57**, 9736–9744. (doi:10.1080/19443994.2015.1030777)
98. Khezami L, Taha KK, Amami E, Ghiloufi I, El ML. 2016 Removal of cadmium (II) from aqueous solution by zinc oxide nanoparticles: kinetic and thermodynamic studies. *Desalin Water Treat.* **62**, 346–354. (doi:10.5004/dwt.2016.0196)
99. Cui H, Li Q, Gao S, Ku J. 2012 Strong adsorption of arsenic species by amorphous zirconium oxide nanoparticles. *J. Ind. Eng. Chem.* **18**, 1418–1427. (doi:10.1016/j.jiec.2012.01.045)
100. Hu Q, Liu Y, Gu X, Zhao Y. 2017 Adsorption behavior and mechanism of different arsenic species on mesoporous $MnFe_2O_4$ magnetic nanoparticles. *Chemosphere* **181**, 328–336. (doi:10.1016/j.chemosphere.2017.04.049)
101. Jian M, Liu B, Zhang G, Liu R, Zhang X. 2015 Adsorptive removal of arsenic from aqueous solution by zeolitic imidazolate framework-8 (ZIF-8) nanoparticles. *Colloids Surf. A Physicochem. Eng. Asp.* **465**, 67–76. (doi:10.1016/j.colsurfa.2014.10.023)
102. Tuutijärvi T, Lu J, Sillanpää M, Chen G. 2009 As (V) adsorption on maghemite nanoparticles. *J. Hazard. Mater.* **166**, 1415–1420. (doi:10.1016/j.jhazmat.2008.12.069)
103. Feng L, Cao M, Ma X, Zhu Y, Hu C. 2012 Superparamagnetic high-surface-area Fe_3O_4 nanoparticles as adsorbents for arsenic removal. *J. Hazard. Mater.* **217–218**, 439–446. (doi:10.1016/j.jhazmat.2012.03.073)
104. Ojea-Jiménez I, López X, Arbiol J, Puntes V. 2012 Citrate-coated gold nanoparticles as smart scavengers for mercury (II) removal from polluted waters. *ACS Nano.* **6**, 2253–2260. (doi:10.1021/nn204313a)
105. Sumesh E, Bootharaju MS, Pradeep AT. 2011 A practical silver nanoparticle-based adsorbent for the removal of Hg^{2+} from water. *J. Hazard. Mater.* **189**, 450–457. (doi:10.1016/j.jhazmat.2011.02.061)
106. Adio SO, Azeem R, Chanabsha B, BoAli AAK, Essa M, Alsaadi A. 2018 Silver nanoparticle-loaded activated carbon as an adsorbent for the removal of mercury from Arabian gas-condensate. *Arab. J. Sci. Eng.* **44**, 6285–6293. (doi:10.1007/s13369-018-3682-4)
107. Ahmadi M, Foladivanda M, Jafarzadeh N, Ramavandi B, Kakavandi B. 2017 Synthesis of chitosan zero-valent iron nanoparticles-supported for cadmium removal: characterization, optimization and modeling approach. *J. Water Supply Res. Technol.* **66**, 116–130. (doi:10.2166/aqua.2017.027)
108. Jabeen H, Kemp KC, Chandra V. 2013 Synthesis of nano zerovalent iron nanoparticles graphene composite for the treatment of lead contaminated water. *J. Environ. Manage.* **130**, 429–435. (doi:10.1016/j.jenvman.2013.08.022)
109. Chowdhury SR, Yanful EK. 2013 Kinetics of cadmium (II) uptake by mixed maghemite-magnetite nanoparticles. *J. Environ. Manage.* **129**, 642–651. (doi:10.1016/j.jenvman.2013.08.028)
110. Chen K *et al.* 2017 Removal of cadmium and lead ions from water by sulfonated magnetic nanoparticle adsorbents. *J. Colloid Interface Sci.* **494**, 307–316. (doi:10.1016/j.jcis.2017.01.082)
111. Rahmanzadeh L, Ghorbani M, Jahanshahi M. 2016 Effective removal of hexavalent mercury from aqueous solution by modified polymeric nanoadsorbent. *J. Water Environ. Nanotechnol.* **1**, 1–8. (doi:10.7508/jwent.2016.01.001)
112. Rahimi S, Moattari RM, Rajabi L, Ashraf A, Keyhani M. 2015 Iron oxide/hydroxide (alpha, gamma-FeOOH) nanoparticles as high potential adsorbents for lead removal from polluted aquatic media. *J. Ind. Eng. Chem.* **23**, 33–43. (doi:10.1016/j.jiec.2014.07.039)
113. Giraldo L, Erto A, Moreno-piraja JC. 2013 Magnetite nanoparticles for removal of heavy metals from aqueous solutions: synthesis and characterization. *Adsorption* **19**, 465–474. (doi:10.1007/s10450-012-9468-1)
114. Contreras AR, García A, González E, Casals E, Puntes V, Sanchez A, Font X, Recillas S. 2012 Potential use of CeO_2, TiO_2 and Fe_3O_4 nanoparticles for the removal of cadmium from water. *Desalin Water Treat.* **41**, 296–300. (doi:10.1080/19443994.2012.664743)
115. Rajput S, Pittman CU, Mohan D. 2016 Magnetic magnetite (Fe_3O_4) nanoparticle synthesis and applications for lead (Pb^{2+}) and chromium (Cr^{6+}) removal from water. *J. Colloid Interface Sci.* **468**, 334–346. (doi:10.1016/j.jcis.2015.12.008)
116. Wang J, Zheng S, Shao Y, Liu J, Xu Z, Zhu D. 2010 Amino-functionalized Fe_3O_4@SiO_2 core – shell magnetic nanomaterial as a novel adsorbent for aqueous heavy metals removal. *J. Colloid Interface Sci.* **349**, 293–299. (doi:10.1016/j.jcis.2010.05.010)
117. Kumar S, Nair RR, Pillai PB, Gupta SN, Iyengar MAR, Sood AK. 2014 Graphene oxide–$MnFe_2O_4$ magnetic nanohybrids for efficient removal of lead and arsenic from water. *ACS Appl. Mater. Interfaces* **6**, 17 426–17 436. (doi:10.1021/am504826q)
118. Dai S *et al.* 2019 Preparation of core-shell structure Fe_3O_4@C@MnO_2 nanoparticles for efficient elimination of U(VI) and Eu(III) ions. *Sci. Total Environ.* **685**, 986–996. (doi:10.1016/j.scitotenv.2019.06.292)
119. Moattari RM, Rahimi S, Rajabi L, Derakhshan AA, Keyhani M. 2014 Statistical investigation of lead removal with various functionalized carboxylate ferroxane nanoparticles. *J. Hazard. Mater.* **283**, 276–291. (doi:10.1016/j.jhazmat.2014.08.025)
120. Huang Y, Keller AA. 2015 EDTA functionalized magnetic nanoparticle sorbents for cadmium and lead contaminated water treatment. *Water Res.* **80**, 159–168. (doi:10.1016/j.watres.2015.05.011)
121. Zhang S, Zhang Y, Liu J, Xu Q, Xiao H, Wang X, Xu H, Zhou J. 2013 Thiol modified Fe_3O_4@SiO_2 as a robust, high effective, and recycling magnetic sorbent for mercury removal. *Chem. Eng. J.* **226**, 30–38. (doi:10.1016/j.cej.2013.04.060)
122. Gong J, Chen L, Zeng G, Long F, Deng J, Niu Q, He X. 2012 Shellac-coated iron oxide nanoparticles for removal of cadmium (II) ions from aqueous solution. *J. Environ. Sci.* **24**, 1165–1173. (doi:10.1016/S1001-0742(11)60934-0)
123. Devi V, Selvaraj M, Selvam P, Kumar AA, Sankar S, Dinakaran K. 2017 Preparation and characterization of CNSR functionalized Fe_3O_4 magnetic nanoparticles: an efficient adsorbent for the removal of cadmium ion from water. *Biochem. Pharmacol.* **5**, 4539–4546. (doi:10.1016/j.jece.2017.08.036)
124. Tabesh S, Davar F, Loghman-Estarki MR. 2017 Preparation of γ-Al_2O_3 nanoparticles using modified sol-gel method and its use for the adsorption of lead and cadmium ions. *J. Alloys Compd.* **730**, 441–449. (doi:10.1016/j.jallcom.2017.09.246)
125. Sheela T, Nayaka YA, Viswanatha R, Basavanna S, Venkatesha TG. 2012 Kinetics and thermodynamics studies on the adsorption of Zn(II), Cd(II) and Hg(II) from aqueous solution using zinc oxide nanoparticles. *Powder Technol.* **217**, 163–170. (doi:10.1016/j.powtec.2011.10.023)
126. Pala IR, Brock SL. 2012 ZnS nanoparticle gels for remediation of Pb^{2+} and Hg^{2+} polluted water. *ACS Appl. Mater. Interfaces* **4**, 2160–2167. (doi:10.1021/am3001538)
127. Gong Y, Tang J, Zhao D. 2016 Application of iron sulfide particles for groundwater and soil remediation: a review. *Water Res.* **89**, 309–320. (doi:10.1016/j.watres.2015.11.063)
128. Patel K, Singh N, Nayak JM, Jha B, Sahoo SK, Kumar R. 2018 Environmentally friendly inorganic magnetic sulfide nanoparticles for efficient adsorption-based mercury remediation from aqueous solution. *ChemistrySelect* **3**, 1840–1851. (doi:10.1002/slct.201702851)

129. Kromah V, Zhang G. 2021 Aqueous adsorption of heavy metals on metal sulfide nanomaterials: synthesis and application. *Water* **13**, 1843. (doi:10.3390/w13131843)
130. Lisha KP, Pradeep T. 2009 Towards a practical solution for removing inorganic mercury from drinking water using gold nanoparticles. *Gold Bull.* **2**, 144–152. (doi:10.1007/BF03214924)
131. Rane AV, Kanny K, Abitha VK, Thomas S. 2018 Methods for synthesis of nanoparticles and fabrication of nanocomposites. In *Synthesis of inorganic nanomaterials*. Woodhead Publishing., ISBN 978-0-08-101975-7, Elsevier Ltd.
132. Marimón-bolívar W, González EE. 2019 Glutathione@Fe_3O_4 nanoparticles as efficient material for the adsorption of mercury(II) from water at low concentrations. *Glob. J. Sci. Front. Res.* **1**, 11–24.
133. Pearson RG. 1963 Hard and soft acids and bases. *J. Am. Chem. Soc.* **85**, 3533–3539. (doi:10.1021/ja00905a001)
134. Zhu Y, He X, Xu J, Fu Z, Wu S, Ni J, Hu B. 2021 Insight into efficient removal of Cr(VI) by magnetite immobilized with *Lysinibacillus* sp. JLT12: mechanism and performance. *Chemosphere* **262**, 127901. (doi:10.1016/j.chemosphere.2020.127901)
135. Hofacker AF, Voegelin A, Kaegi R, Kretzschmar R. 2013 Mercury mobilization in a flooded soil by incorporation into metallic copper and metal sulfide nanoparticles. *Environ. Sci. Technol.* **47**, 7739–7746. (doi:10.1021/es4010976)